agso RESEARCH NEWSLETTER

'Geoscience for Australia's Future'

Number 25 November 1996

# Re-evaluating the structure of Broken Hill

## Implications for mineral exploration and the interpretation of airborne magnetic data

*George M. Gibson[1], David W. Maidment[1], & Richard Haren[1]*

**As part of the Broken Hill Exploration Initiative, AGSO recently undertook detailed structural mapping at a number of key locations in the Broken Hill region (Fig. 1) in order to:**

- evaluate any new structures revealed by the data acquired during an AGSO aeromagnetic survey last year;
- better understand the relationship between structure and the aeromagnetic anomalies; and
- assess the extent to which the anomalies permit an improved interpretation of the regional structure and/or stratigraphy.

An added impetus for the mapping was the publication in early 1995 of a new structural interpretation for Broken Hill (White et al. 1995: Transactions of the Institution of Mining & Metallurgy, 104, B1–B17) that identifies several discrete thrust packages. This new interpretation is controversial (cf. Stevens 1996 and White et al. 1996: Transactions of the Institution of Mining & Metallurgy, 105, B89–B98), but, if validated, has major implications not only for the regional stratigraphy of Broken Hill but also for mineral exploration in general around the region.

### Previous structural interpretations

Structural models for the Broken Hill region largely reflect work undertaken in the late 1970s (e.g., Laing et al. 1978: Economic Geology, 73, 1112–1136; Marjoribanks et al. 1980: Precambrian Research, 13, 209–240). They incorporate a series of major northeast-trending nappes (D1) which were refolded about more upright D2 folds. Nappe formation coincided with both amphibolite- to granulite-facies metamorphism and regional stratigraphic overturning with little or no disruption to the lithological package. D2 deformation also occurred during high-grade metamorphism and was followed by further folding (D3) and development of the many retrograde shear zones that are conspicuous on 1:25 000 geological maps of the region.

The retrograde shear zones disrupt the regional stratigraphy, and have been the subject of several recent studies (e.g., White et al. 1995). These authors challenged the interpretation of early recumbent D1 structures. They reinterpreted the Broken Hill Block as a series of discrete thrust packages, each with its own internal structural geometry and separated from its neighbours by high-angle thrust-faults. In their view, the retrograde shear zones were much older structures that had been reactivated during later deformation. Indeed, in their view, these shear zones are former thrusts which first became active during the earlier high-grade metamorphism. Only through careful investigation of the associated structures, mineralogy, and kinematic indicators was it possible to determine both the original character of these shear zones and their associated sense of displacement. In contrast to many earlier investigators, they argued that continuity of the regional stratigraphy cannot be assumed, particularly between thrust-sheets.

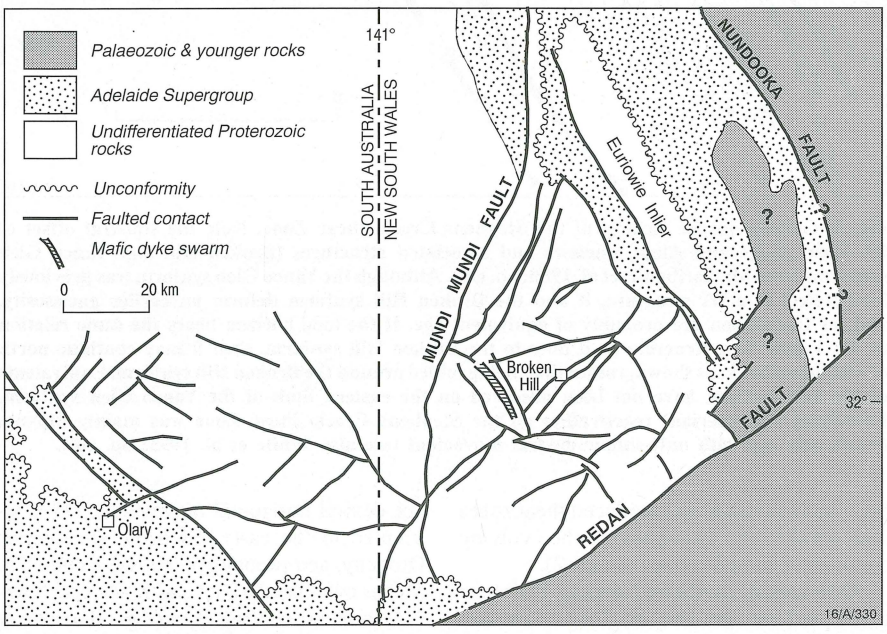


**Fig. 1. Simplified geology, Broken Hill region. Note the predominance of northwest- and northeast-trending structures which are parallel and orthogonal to the former Late Proterozoic Gondwanan continental margin (Fig. 2). Late Proterozoic sedimentary basins (Adelaidean) and the Broken Hill dyke swarm are similarly oriented parallel to the continental margin.**


**Fig. 2. Lineaments representing the inferred Proterozoic Gondwanan continental margin superimposed on a greyscale image of total magnetic intensity with illumination from the northeast, eastern Australia.**

*Table of Contents on page 2*

AGSO

Australian Geological Survey Organisation

A research organisation of the Department of Primary Industries & Energy

AGSO JUBILEE 1946-96

## Results of the recent AGSO structural mapping

Structural mapping undertaken by AGSO, combined with on-site investigation of various aeromagnetic anomalies over the last year, confirms the structural complexity of the retrograde shear zones, and the need to re-examine their role in the structural evolution of Broken Hill. Evidence of earlier high-grade metamorphism and deformation is indeed widely preserved within many of the shear zones, although an intimate knowledge of the regional geology is necessary to determine whether the earlier structures are peculiar to the shear zones or represent elements of country rock which were incompletely overprinted during later shearing. In order to address these problems, structural mapping by AGSO was directed at an understanding of both the regional structure and the shear zones. A preliminary account of our results is presented below.

Amphibolite–granulite facies metamorphism in the Proterozoic rocks of Broken Hill (Willyama Supergroup) was accompanied by multiple deformation (D1–D3). The last of these produced regionally extensive upright folds with vertical to steeply dipping northeast-trending axial-plane fabrics and associated transposition structures. Subsequent deformation (D4–D5), accompanied by lower-grade metamorphism, was mainly shear-related. The retrograde shear zones originated during the D4 deformation. Unlike White et al. (1995), we found no evidence for earlier southwest-directed thrust-faulting along them. Rather, we attribute the origin and earliest movement on the retrograde shear zones to continental rifting and the Late Proterozoic separation of Laurentia from Gondwana. The D4 deformation is related to the breakup of Rodinia, and produced shear zones both parallel and orthogonal to the evolving continental margin (Figs. 1 and 2).

Orthogonal, northeast-trending D4 shear zones predominate. They originated as strike-slip faults that locally truncate, but more commonly parallel, the D3 regional fabric, and thus reflect a degree of control by the pre-existing structures. Shear zones with this orientation originally had a sinistral sense of displacement, as evidenced by suitably offset marker horizons (e.g., Rasp Ridge Gneiss; Fig. 3), and include the Redan Fault (Fig. 1). During later deformation (D5), many of these shear zones were reactivated as northwest-directed thrust-faults (with minor dextral horizontal movement). D5 is attributed to the early Paleozoic Delamerian Orogeny, and probably occurred around 520 Ma, as evidenced by several K–Ar and $^{40}Ar$–$^{39}Ar$ mineral cooling ages (e.g., Harrison & McDougall 1981: Earth and Planetary Science Letters, 55, 123–149). Thus, in common with White et al.(1995: op. cit.), we recognise a late episode of northwest-directed thrust-faulting, but differ in our interpretation of the earlier kinematic picture for the northeast-trending retrograde shear zones.

The northwest-trending D4 shear zones possibly originated as normal faults, and might have been associated with crustal thinning. They not only facilitated dyke intrusion

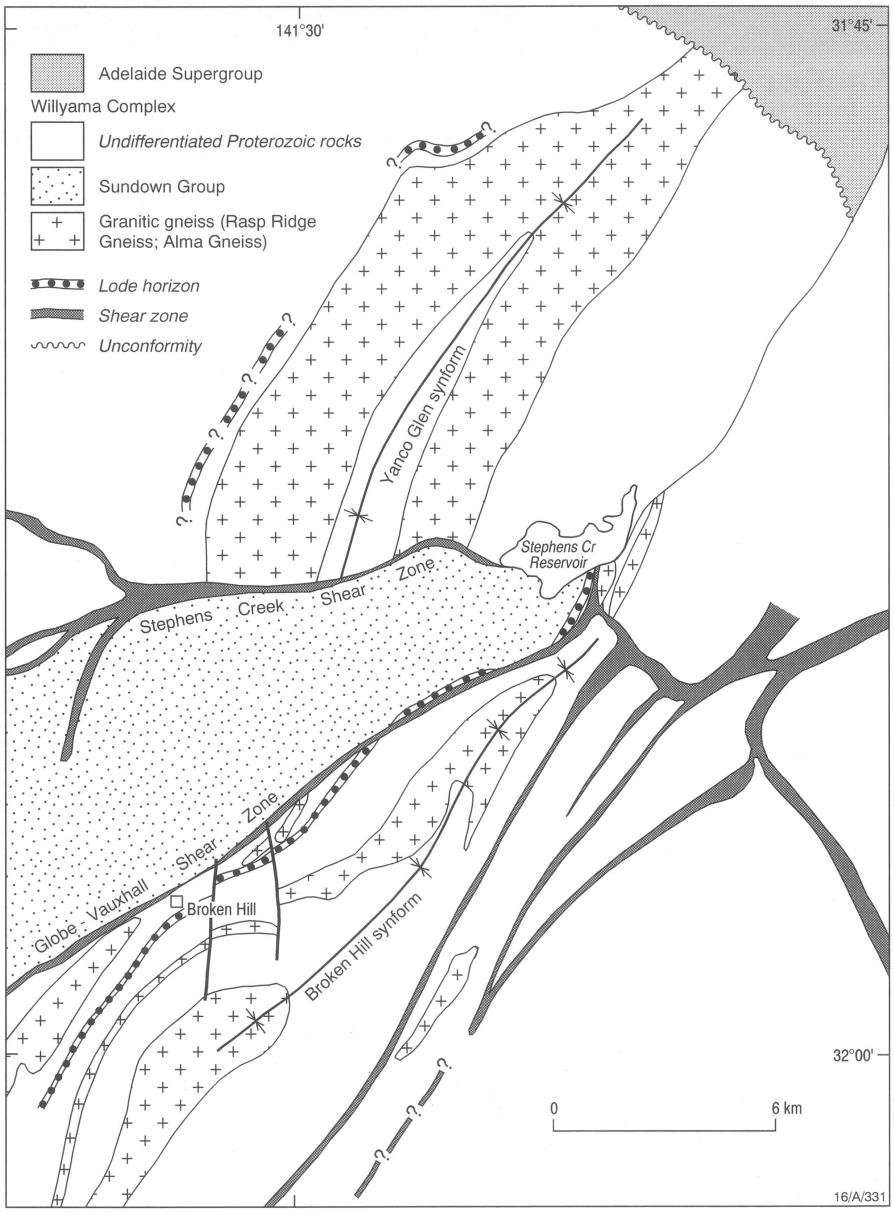


**Fig. 3. Geology in the vicinity of the Stephens Creek Shear Zone. Note the sinistral offset of the Rasp Ridge and Alma Gneisses and associated structures (Broken Hill and Yanco Glen synforms from Marjoribanks et al. 1980: op. cit.). Although the Yanco Glen synform was previously interpreted as a D1 structure, it and the Broken Hill synform deform an earlier gneissosity, and for this reason are probably of equivalent age. If the lode horizon bears the same relation to the Yanco Glen structure as it does to the Broken Hill synform, then it may continue north of Stephens Creek, as shown, rather than being folded around the Broken Hill synform. Equivalents of the lode horizon have not been observed on the eastern limb of the Yanco Glen synform. Late-stage (Delamerian) reactivation on the Stephens Creek Shear Zone was mainly dip-slip (south side up) with only minor dextral movement (see also White et al. 1995: op. cit.).**

# In this issue:

in the Broken Hill region but influenced sedimentation patterns in the Upper Proterozoic–lower Palaeozoic Adelaide Supergroup. Late Proterozoic sedimentary basins in the Broken Hill and adjacent Olary Blocks trend northwest, parallel to the former continental margin (Fig. 2), and commonly exhibit a marked asymmetry consistent with deposition of the Adelaide Supergroup in a series of fault-angle depressions or half-grabens (Preiss 1987: Geological Survey of South Australia, Bulletin 53). During the onset of the Delamerian Orogeny, sediments in these basins were intensely folded, and the D4 normal faults reoriented into their present steep attitudes.

## Implications for mineral exploration

### Whither the line of lode?

The structural analysis of the retrograde shear zones presented above has important implications for mineral exploration and the interpretation of the aeromagnetic data. The original character and sense of movement of the shear zones clearly have been masked by later reactivation during the Delamerian Orogeny. This is particularly true of the northeast-trending zones, which truncate or disrupt a number of important marker horizons near the mine sequence — including the Rasp Ridge Gneiss — and also might have been responsible for terminating the lode horizon south of Stephens Creek reservoir (Fig. 3).

The major structure shown on 1:25 000 maps of the reservoir area is the Stephens Creek Shear Zone. We interpret the precursor of this structure to have been a strike-slip fault that sinistrally offset the Rasp Ridge Gneiss (Fig. 3). A corollary to this interpretation is that the mine sequence, like the Rasp Ridge Gneiss, might continue north of the Stephens Creek Shear Zone. Previously, the lode horizon was expected to have been folded around the Broken Hill synform, leading many companies to direct their mineral exploration along the southern limb of the structure.

Past difficulties with the Stephens Creek Shear Zone stem from the observation that its best developed and most conspicuous kinematic indicators require a dextral sense of displacement. However, this interpretation presupposes that there has been only one episode of significant movement on the shear zone. In the analysis presented here, the kinematic indicators relate only to the Delamerian Orogeny, whose effects have masked the earlier history of the shear zone. The earlier kinematic history is more readily discerned from offsets in the regional stratigraphy.

## Origin of aeromagnetic anomalies

Many of the more prominent northeast-trending aeromagnetic anomalies appear to coincide with the D4 shear zones. These anomalies are not only discordant to the regional stratigraphy but some of them cut across the lithological layering at high angles. Moreover, whereas retrograde metamorphism associated with the Delamerian reactivation of the D4 shear zones was commonly magnetite-destructive, events during the D4 deformation appear to have promoted the crystallisation of magnetite. Ground surveys with hand-held magnetic susceptibility meters support these observations. In common with several previous studies (e.g., McIntyre 1979: Bulletin of the Society of Australian Exploration Geophysicists, 10, 42–53), we conclude that many aeromagnetic anomalies in the Broken Hill region are structurally, rather than stratigraphically, controlled, and evidently formed rather late in the tectonic evolution of the Willyama Supergroup. Other anomalies appear to coincide with particular lithologies (e.g., some amphibolites), whereas others bear no obvious relationship to either the stratigraphy or regional structure. These relations indicate that the magnetic anomalies may not all be of the same age or origin. Further work on their origin is in progress.

[1] Minerals Division, Australian Geological Survey Organisation, GPO Box 378, Canberra, ACT, 2601: tel. +61 6 249 9727 (GMG), +61 6 249 9389 (DWM), +61 6 249 9586 (RH); fax +61 6 249 9983; e-mail ggibson@agso.gov.au, dmaidmen@agso.gov.au, rharen@agso.gov.au.

# If only Newton had had AGSO's FieldPad

*Murray Hazell[1], Richard Blewett[1], & Jeff Bailey[2]*

**AGSO, in conjunction with Resource Industry Associates (RIA), has developed the AGSO FieldPad — a digital version of their popular structured field notebooks. The FieldPad operates on an Apple Newton palmtop computer (120 or 130) and is set to greatly increase the speed and efficiency of production of Geographic Information Systems (GISs) in AGSO.**

## The influence of GIS on data acquisition

GISs and digital data have revolutionised the way geological data can be presented and used. GISs not only permit the integration and interrogation of many layers of data, they also allow the detail at which the data were captured to be preserved. No longer do purchasers of geoscientific data have to be satisfied with a synthesis and generalisation of geological information, as they do for the presentation of data on two-dimensional paper maps. All data collected for a mapping program can be presented, at the original compilation scale in a GIS, which may include the geologist's field notes. Information contained in the geologist's field notes is an important aid for interpreting other data sets, and should be made available within the GIS, thus enabling new themes to be generated from them — for example, alteration maps based on field observations of alteration assemblages.

Data account for much of the cost of a GIS. Data are expensive to buy and even more expensive to capture. They are also liable to human error, especially during the process of transcription (Fairall 1994: GIS User, 8, 43–45). Setting up databases for integrating field observations within the demands of a GIS can help to minimise some of these costs and reduce the error factor. Structured field notebooks and coded attributes are two strategies which AGSO has adopted to improve the process of data collection. Not only do such facilities increase the speed of data entry, equally importantly, they ensure that fundamental data/information for an effective GIS are collected at each site (Blewett 1993: AGSO Record 1993/46) — for example, a geographic coordinate, an indication of its positional accuracy, and, if the location was recorded on a GPS, which datum the GPS was set on. Also, structured field notebooks overcome

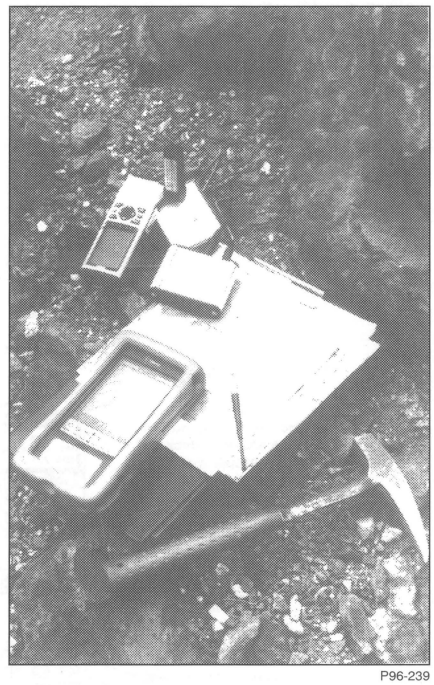

P96-239

**Fig. 4. AGSO FieldPad software operating on an Apple Newton palmtop computer is streamlining the collection of field data in AGSO.**

[1] Minerals Division, Australian Geological Survey Organisation, GPO Box 378, Canberra, ACT, 2601: tel. +61 6 249 9375 (MH), +61 6 249 9713 (RB); fax +61 6 249 9983; e-mail mhazell@agso.gov.au, rblewett@agso.gov.au.

[2] Resource Industry Associates, 538 Brunswick Street, North Fitzroy, Victoria 3068; tel. +61 3 9482 4945; fax +61 3 9482 4956; http://www.ozemail.com.au/~ria.

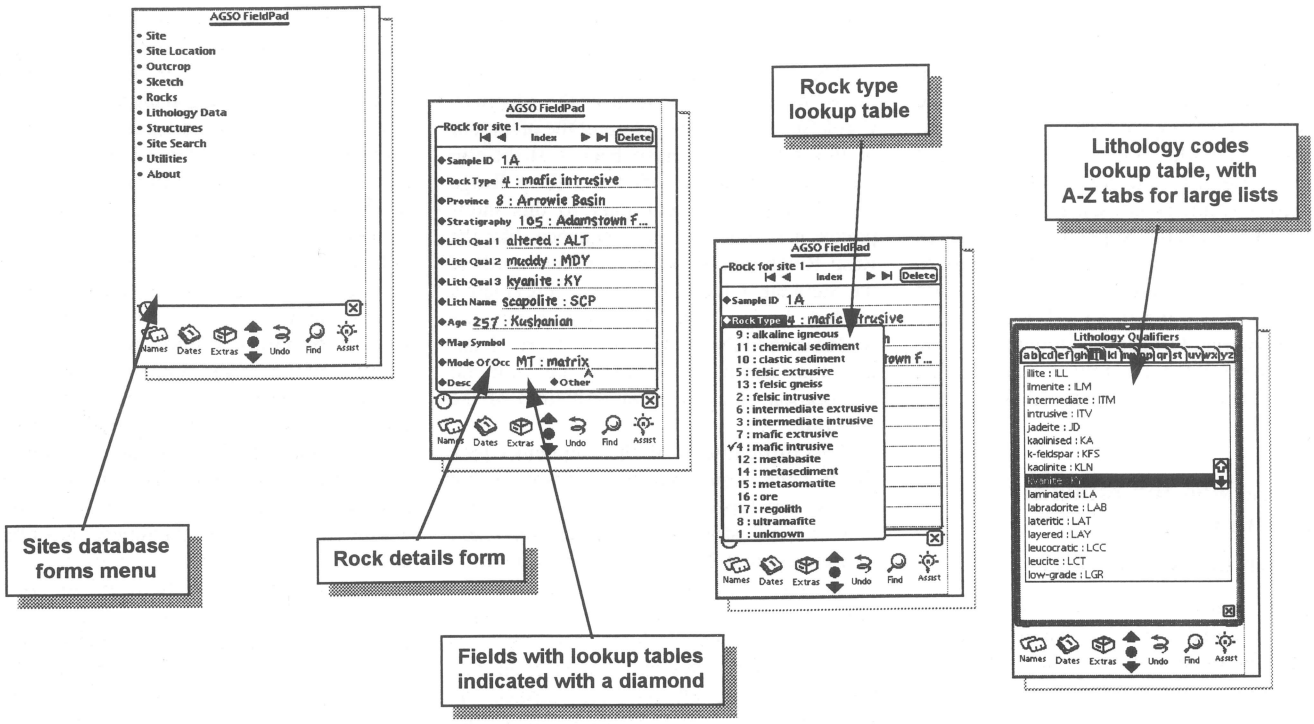


**Figure 5. An example of some screens from AGSO's FieldPad. Note the use of pull-down menus to assist data choice and accurate simple data entry.**

the geologists' tendency to bias their data collection towards their own speciality; reduce the tendency to synthesise excessively the description of an outcrop; and encourage instead the recording of individual outcrop features for later storage as searchable attributes in a database. They remind the geologist to record information at the outcrop that is of use to others working on the project. Thus, magnetic susceptibility readings can aid aeromagnetic interpretation; spectrometer measurements of the amounts of radiogenic minerals can help airborne radiometric interpretation; and a description of vegetation can assist an understanding of Landsat Thematic Mapper data.

Digital data capture of geological descriptions is not new. For example, drillcore is commonly logged digitally at mine sites. Digital logging packages were developed because of the need to get data quickly and easily into digital 3-D mine graphics programs. Mine packages were moderately easy to develop as they had to cater only for the mine environment, which has a limited number of known attributes. Also, computer portability was not a major impediment, as a PC could be quite easily wheeled along the trays of core. It was easy therefore to obtain machines that were fast and powerful enough to rapidly record such data.

By contrast, similar systems for field mapping have been slow to evolve owing to the many attributes that have had to be catered for, particularly if a system was to be portable around Australia. The increased use of GIS and the requirement to have data available digitally has provided the impetus to develop a digital field-data-capture system. It has spawned AGSO's FieldPad.

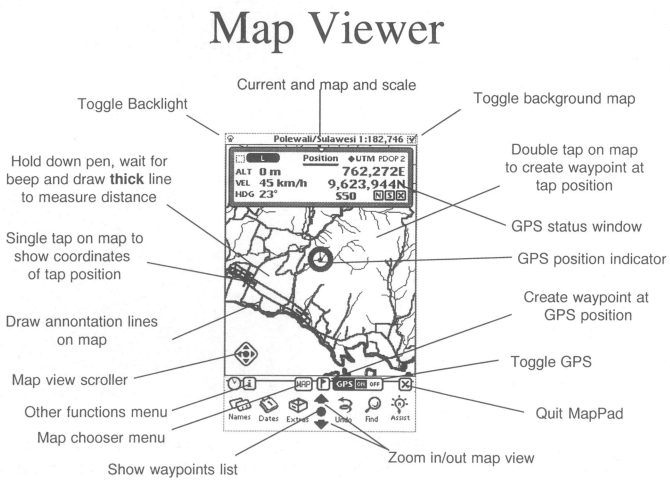


**Fig. 6. An example of the MapPad screen and some features of the package.**

## AGSO's FieldPad

Operating from a small powerful palmtop Apple Newton computer (Fig. 4), AGSO's FieldPad constitutes a portable system designed to make all of AGSO's field database attributes available for a geologist to use in the field. The FieldPad system represents an extension of the structured field notebooks: it enables the data to be entered digitally at the source, thereby removing the need to spend large amounts of additional time transcribing them into a digital database.

The geologist uses a pen to control the Newton and enter data via a touch-sensitive screen. The FieldPad uses the same structure as AGSO's OZROX corporate field database (Ryburn et al. 1993, 1995: AGSO Records 1993/49, 1995/79), and most of the data are entered via selections made from pull-down menus, a facility that speeds data entry and eliminates errors (Fig. 5). Some free text fields are available in the Newton, whose character-recognition software allows geologists to enter their descriptions freehand. Field sketches can also be stored in the Newton, and downloaded with the field-site descriptions into a database for display in the office.

Another feature of the FieldPad which makes it superior to paper notebooks is its ability to display georeferenced vector images of topographic and/or geological maps, or geophysical interpretations. MapPad, developed solely by RIA, links a GPS position via an infra-red connection to a variety of maps (displayed on the screen) in real time,

allowing users to navigate easily to particular outcrops or interpreted features (Fig. 6). Linking the database and map with the GPS enables positions to be captured directly, thus eliminating the risk of transcription errors. RIA also provides a service for importing .DXF files into the MapPad map package. Now users can create their own maps from an add-on module in the TerraScan PC/Windows software. Different line attributes can be encoded to enhance the display, and a number of maps or scales of maps may be loaded (Fig. 6).

All new data are stored on 2- or 4-Mb flash cards, which can be removed for security/safety. The Newton communicates with both PC (Windows) and Macintosh computers by RS232 serial cables or infra-red beam for down-/uploading of data and maps and customised look-up tables. The Newton operates on 4AA batteries (nicads or disposable) that run for about a week. The infra-red connection from the GPS requires a 4AA power pack, and is very economical. Power can also be supplemented by 12-V cigarette-lighter points for vehicle use. The Newton is shock-protected by a rubber boot, but currently is not waterproof.

## Discussion

The creation of GIS data sets requires a new approach to geological data capture. Mappers need to recognise that their data can be presented to clients at the scale at which they were captured. Indeed this degree of detail is now being demanded by exploration companies as their level of GIS sophistication increases. Providing accurate data at capture scale puts particular pressure on data providers, and also vastly increases the amount of data being processed. Recognition of the need for accuracy in raw-data collection will greatly speed the process of building a successful GIS. AGSO's FieldPad makes this easier by reducing the capture of field notes to a single step, eliminating transcription errors.

# New insights to the evolution of the Bass Basin

*Peter J. Gunn[1], Jane Mitchell[1], & Tony (A.) Meixner[1]*

**The Bass Basin, a failed Mesozoic rift located offshore between Tasmania and Victoria, was formed as a result of extension during the separation of the Australian and Antarctic continents. Integrations of the first available complete aeromagnetic coverage of the basin, new gravity data computed from satellite measurements, and seismic, drillhole, and**

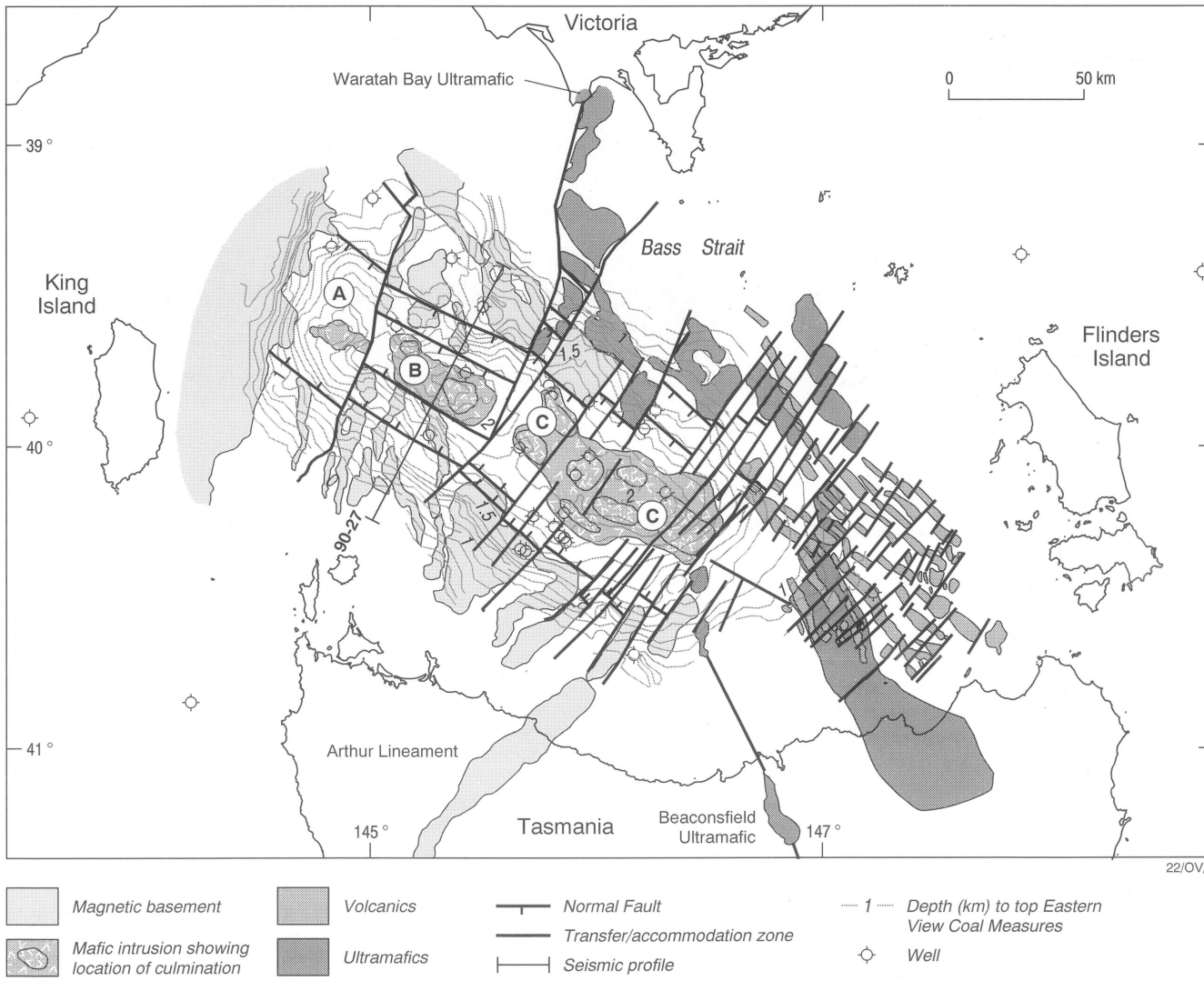


**Fig. 7. Synthesised interpretation showing the major elements of the Bass Basin. Magnetic basement units have been ruptured and separated by extension accommodated by northeast-trending transfer-type faults. Three compartments (A, B, C) are identified as having undergone different amounts of extension, which increases southeastwards. Thickness variations in the sag-phase deposits (post-Eastern View Coal Measures; from Williamson et al. op. cit.) reflect the compartmentalisation of the extension.**

[1] Minerals Division, Australian Geological Survey Organisation, GPO Box 378, Canberra, ACT 2601; tel. +61 6 249 9226 (PJG), +61 6 249 9244 (JM) +61 6 249 9636 (AM); fax +61 6 249 9986; e-mail pgunn@agso.gov.au, jmitchel@agso.gov.au.

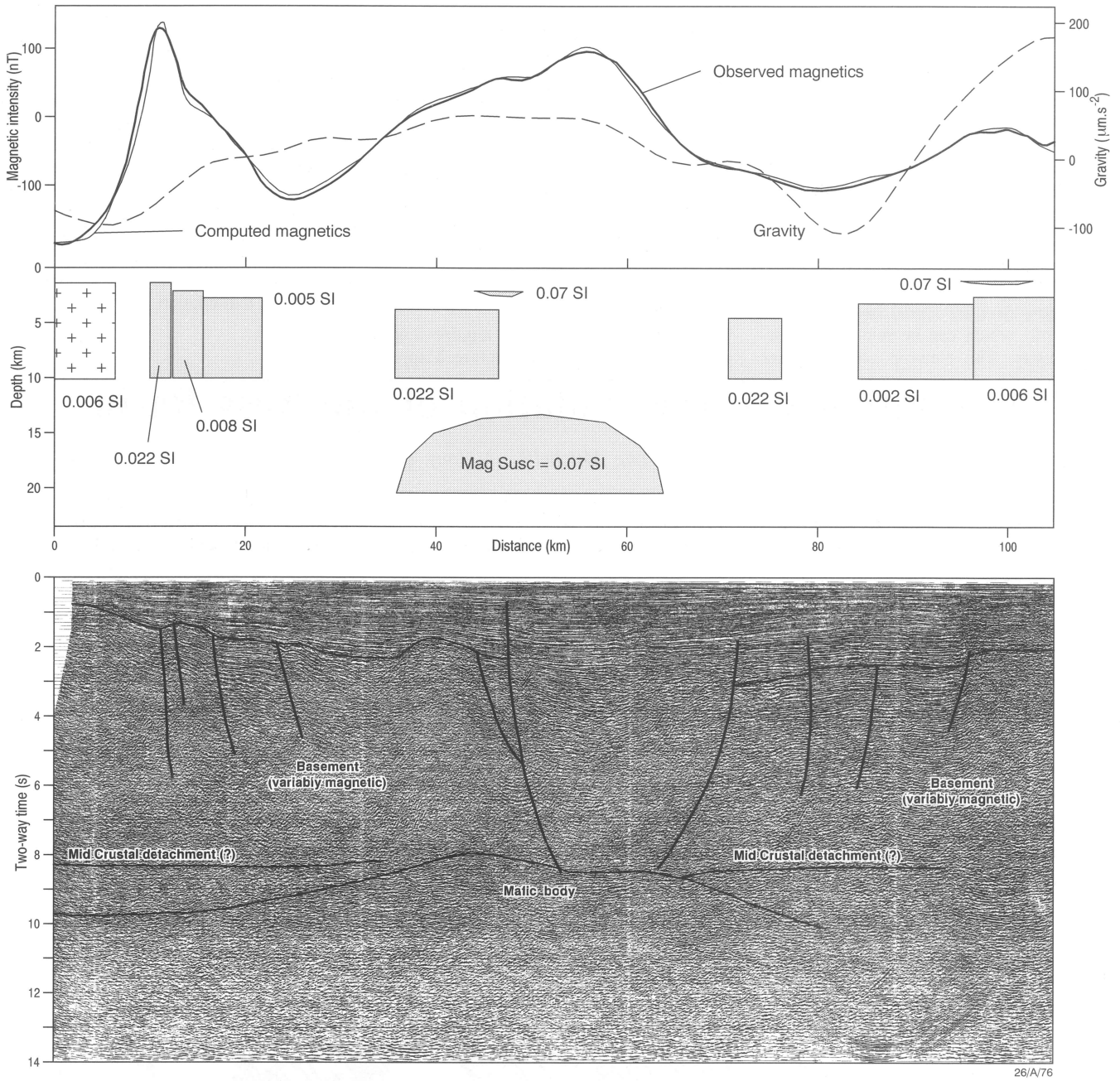


**Fig. 8. Seismic, magnetic, and gravity data for profile 90-27 (see Fig. 7 for location). Magnetic modelling indicates a major mafic intrusion (magnetic susceptibility 0.07 SI units) beneath the Bass Basin. This intrusive mass is evident in seismic reflection data and corresponds to a gravity high.**

**outcrop-geology data allow a new interpretation of the structure and evolutionary history of the basin (Fig. 7).**

## Previous work

According to Williamson et al. (1985: APEA Journal, 25, 362–381), the main depocentre of the Bass Basin appears to overlie an area where the Proterozoic basement was fractured and dislocated by northeastward–southwestward tensional forces to such an extent that their corresponding portions on the northern and southern basin margins are now separated by as much as 60 km. This fracture and extension is thought to have occurred in the brittle upper crust along a large listric fault which soled out into a regional subhorizontal detachment plane at a depth of about 15 km.

This model is consistent with features that Willcox et al. (1993: 'Proceedings of the Gippsland Basin Symposium, Melbourne, 22–23 June 1992', Australasian Institute of Mining & Metallurgy + Petroleum Exploration Society of Australia, Melbourne, 93–114) inferred from detailed deep seismic reflection and refraction data to explain the geometry and origin of the Gippsland Basin, which is located 150 km to the northwest of the Bass Basin. The Gippsland Basin is generally regarded as having been initiated contemporaneously with the Bass Basin as a result of the same extensional tectonic event — viz., the separation of the Australian and Antarctic continents (Etheridge et al. 1987: in Beaumont & Tankard (editors), 'Sedimentary basins and basin forming mechanisms', Canadian Society of Petroleum Geologists, Memoir 12, 147–162).

## Implications of the newly integrated data sets

Willcox et al. recognised a continuation of the detachment plane, apparently at or near the junction between upper brittle crust and ductile lower crust, from the Gippsland Basin to the Bass Basin. The rifting of the upper crust in the Bass Basin apparently created a depression with a generalised rectangular plan, up to 60 km wide, that the sediments of the Bass Basin subsequently filled.

The bases for interpreting the fracturing and rifting of the upper crust in the Bass Basin are:

- the abrupt termination of the magnetic basement units on the northern and southern sides of the basin;
- jigsaw-type matches between what appear to be fragments of corresponding magnetic units on the northern and southern borders of the interpreted zone of rupturing; and
- the complete absence of any indication in the magnetic data of any continuation of these magnetic basement units at depth across the floor of the basin.

The interpretation is supported by deep seismic data, particularly along line 90/27, which show no evidence for downfaulted basement below the main sediment depocentre. Subhorizontal reflections, possibly indicating a detachment plane, are apparent in the data of line 90/27 (Fig. 8).

The fracturing of the upper crust, including the basement, as defined by terminations of magnetic basement units, appears to have occurred in directions broadly orthogonal to the northeast–southwest extension direction. The separation of the basement fragments varies along the axis of the basin. The magnetic anomaly pattern in the basement, and the magnetic lineations arising from sources in the sedimentary section, suggest that differential extension between different compartments was accommodated by movement along transfer faults — the type proposed by Etheridge et al. (op. cit) to explain the origin and character of the Bass Basin.

Three main compartments to the extension (A, B, and C in Fig. 7) are apparent from interpreted matches between what appear to be fragments of originally continuous magnetic bodies along adjacent margins of the basin. They exhibit a progressively greater degree of extension towards the southeast. The compartments coincide with three clearly defined areas of differing thickness apparent for the post-Eastern View Coal Measures (sag phase) in an isopach map compiled by Williamson et al. (op. cit.; cf. Fig. 7). These isopach differences reflect contrasting subsidence histories. Compartment C appears to contain subcompartments bounded by transfer-type faults on which less lateral movement has occurred than on the major transfer faults bounding the main compartments. The compartments overlie accumulations of dense magnetic mafic material, evident on 14-second seismic reflection data, which were apparently produced by a mantle-decompression process associated with crustal thinning. The size and degree of development of the mafic bodies appears to accord with the degree of extension. The largest of these mafic bodies displays a symmetry suggesting it has the characteristics of a preserved embryonic oceanic-spreading centre.

The primary controls of the transfer fault locations and directions appear to be basement lithological contacts and/or faults. The abrupt southeastern limit to the basin corresponds to an offshore extension of the Arthur Lineament, which is a linear zone of high-grade metamorphic Proterozoic rocks represented by a distinct intense linear magnetic anomaly. The abrupt northwestern margin of the basin corresponds to the contact between a highly magnetic basement unit, identified as Proterozoic volcanics from field mapping on King Island by M. Roach (University of Tasmania, personal communication 1995), and a wide, less magnetic unit to the east. The boundary between compartments A and B is another junction between magnetic and non-magnetic basement units. The control on the transfer zone between compartments B and C appears to have been a north-striking, strongly magnetic unit which correlations with outcrops of Cambrian greenstones at Waratah Bay (Vic.) suggest is due to a zone of ultramafic rocks.

# The use of X-rays and neutrons to evaluate hydrocarbon generation in petroleum-source rocks

*Andrzej Radlinski*[1]

**The analysis of small-angle scattering of X-rays (SAXS) and neutrons (SANS) provides for the first time an insight into the process of hydrocarbon generation in organic-rich rocks. These techniques are sensitive to the onset of generation, and can distinguish accurately between organic-rich rocks that have generated hydrocarbons and those that have not.**

SAXS and SANS have been used for over two decades to gain insight into the microstructure of various substances, including polymers, colloids, biological tissue, and other materials. For instance, small-angle scattering can provide information about the shape of polymer chains in solution, molecular organisation in liquid crystals, and the structure of biological cell walls. Unlike the better known diffraction methods, SAXS and SANS are sensitive to the large microstructural features ranging in size from about 10 Å to at least 10 μm — that is, from nearly atomic to clearly visible with an optical microscope.

SAXS and SANS are the only non-invasive techniques that can resolve the bulk of a specimen with high resolution. This makes them ideally suited for surveying pores in sedimentary rocks. Even so, small-angle scattering has not been routinely applied to the studies of rocks before. In order to establish the optimal experimental conditions for this new application, it has been necessary to perform a number of collaborative measurements using Australian and some of the best overseas facilities: in Sydney (Australian Nuclear Science & Technology Organisation); in Tsukuba, Japan (Australian National Beam Facility, in collaboration with CSIRO); in Oak Ridge, USA (Oak Ridge National Laboratory); and in Grenoble, France (European Union's Institut Laue-Langevin).

One of the rock characteristics routinely obtained from the small-angle-scattering studies is the specific pore surface (the internal surface area per unit volume of rock). However, the SAXS and SANS techniques are not only sensitive to the detailed shape of the pore space but also to the type of fluid (gas, water, hydrocarbons) that fills the space. This sensitivity is quantified by the contrast value between the rock matrix and the pore-filling fluid. As the contrast depends both on the chemical composition of the rock and the type of radiation used (neutrons or X-rays), the experimental conditions can be optimised for the particular type of rock so that the structural features of interest are best visible.

In a recent AGSO study, SAXS and SANS have been used to address the problem of primary migration in type II organic-matter hydrocarbon-source rocks (Radlinski et al. 1996: Physical Review B, 53(21), 14152–14160). The techniques have been demonstrated to be sensitive enough to monitor the reorganisation of the pore space upon thermal maturation in a natural maturity sequence of shaly source rocks. As the organic matter (dispersed in the inorganic matrix) matures, the onset of the hydrocarbon generation is accompanied by an internal pressure build-up, usually referred to as overpressuring. The rising pressure opens up a network of microfractures, thus providing conduits for the primary migration. This critical moment is reflected in the scattering experiment as a sudden change in the scattering characteristics of the source rock. This change provides a precise measurement of the onset of hydrocarbon generation, and distinguishes the source rocks that have produced hydrocarbons from those that have not.

In a control study of the artificially pyrolysed series of identical type II source rocks, a marked change of scattering contrast was observed at the onset of hydrocarbon generation, in full agreement with the natural maturity series data.

Another study of SAXS and SANS on a natural maturity sequence of coals, as part of the 'Sedimentary basins of eastern Australia' National Geoscience Mapping Accord project, is currently in progress. Future studies will concentrate on marine source rocks in support of the 'North West Shelf' project.

[1] Petroleum & Marine Division, Australian Geological Servey Organisation, GPO Box 378, Canberra, ACT 2601; tel. +61 6 249 9549; fax +61 6 249 9983; e-mail aradlins@agso.gov.au.

# The age of Cu–Au mineralisation, Cloncurry district, Mount Isa Inlier, as determined by $^{40}Ar/^{39}Ar$ dating

*Caroline Perkins[1] & Lesley Wyborn[2]*

**$^{40}Ar/^{39}Ar$ dating of alteration biotite, muscovite, and amphibole from a number of post-peak metamorphic deposits and from hydrothermal alteration systems associated with granitic intrusions in the Williams Batholith, Cloncurry district, Mount Isa Inlier, has revealed the timing of hydrothermal activity and mineralisation. Alteration biotite from the Ernest Henry Cu–Au, Starra Au–Cu, and Mount Elliott Cu–Au deposits; sericite associated with hematite breccias in the Wimberu Granite; muscovite from an albitite pipe which intrudes the Gilded Rose Breccia; and sericite from a granite near Osborne — all give ages which are inferred to be broadly contemporaneous with the late ~1520–1490-Ma phases of the Williams and Naraku Batholiths. At the Osborne Cu–Au deposit, hornblende and biotite alteration products which predate Cu–Au mineralisation give a maximum age of ~1540 Ma for the deposit. Metamorphic minerals near Osborne record an age of ~1590 Ma, which is older than the age indicated for the hydrothermal alteration and the generally accepted ~1530-Ma age of metamorphism in the Mount Isa Inlier. Attempts to date alteration K-feldspar coexisting with sericite was less successful, yielding ages that were up to 300 m.y. younger than the sericite.**

Large world-class Proterozoic Cu–Au deposits occur around late phases of the Williams and Naraku Batholiths (Wyborn 1992: AGSO Research Newsletter 16, 13–16). An association of these deposits with the granites was first postulated by Nye & Rayner (1940: Aerial Geological & Geophysical Survey of Northern Australia, Report 35). More recently, others have suggested that the deposits represent 'exhalation' contemporaneous with their host rocks (Davidson 1992: Economic Geology, 87, 889–912); or that they formed during deformation before the late granites intruded (Laing 1993: Australian Institute of Geoscientists [AIG], Bulletin 13, 17–24). Still others have concurred with the early workers, and suggested that they were synchronous with the emplacement of the late post-deformation granites (Laing 1993: op. cit.; Wyborn & Heinrich 1993: AIG, Bulletin 13, 27–30).

Published U–Pb zircon ages of the post-tectonic granites range from about 1520 to 1490 Ma (Page & Sun 1996: Economic Geology Research Unit [EGRU], James Cook University of North Queensland[JCUNQ], Contribution 55, 95–98):

- for the Naraku Batholith — 1505 ± 5 Ma (Malakoff granite) and 1501 ± 6 Ma (Capsize granodiorite);
- for the Williams Batholith — ca 1520 Ma (Saxby Granite; P. Pollard, JCUNQ, & N. McNaughton, University of Western Australia, personal communication 1996), 1508 ± 4 Ma (Wimberu Granite), and 1493 ± 8 Ma (Yellow Waterhole Granite).

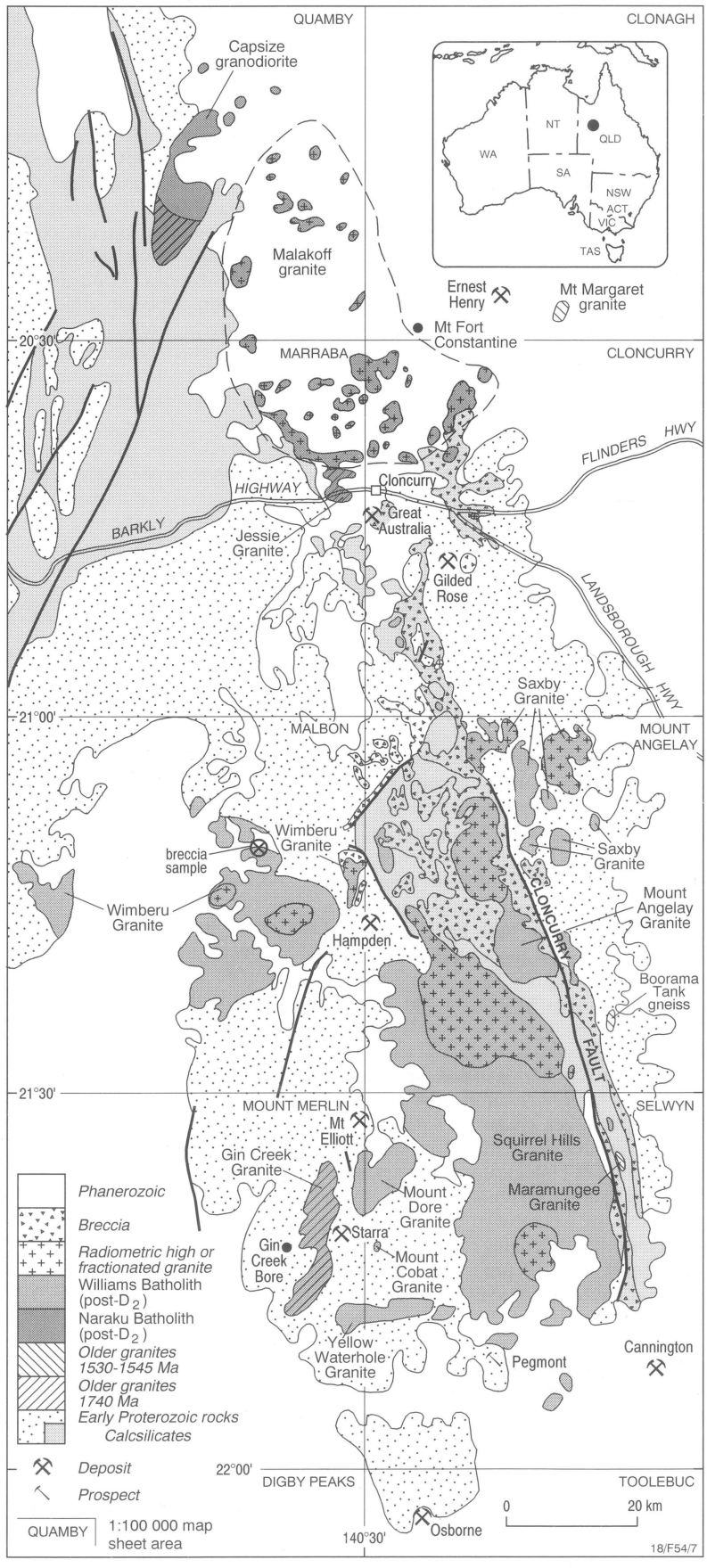


**Fig. 9. Distribution of mineral deposits in the eastern Mount Isa Inlier.**

[1] Formerly Australian National University; now Coal & Minerals Division, Department of Primary Industries & Energy, GPO Box 858, Canberra, ACT 2601; tel. +61 6 272 5780; fax +61 6 272 4965; e-mail caroline_perkins@regate.dpie.gov.au.

[2] Minerals Division, Australian Geological Survey Organisation, GPO Box 378, Canberra, ACT 2601; tel. +61 6 249 9489; fax +61 6 249 9983; e-mail lwyborn@agso.gov.au.

The successful application of $^{40}Ar/^{39}Ar$ dating to hydrothermal alteration in Palaeozoic base-metal deposits in the Tasman Fold Belt (e.g., Perkins et al. 1995: Economic Geology, 85, 1443–1466) encouraged a consortium to initiate a pilot project to apply the same method to late Cu–Au deposits in the Mount Isa Inlier. The project was funded by the provision of a Collaborative Research Grant from the Australian Research Council, and the Australian Minerals Industry Research Association sponsorship of eight companies. Samples were collected in conjunction with AGSO, JCUNQ, and company personnel. The aim of the project was to date (i) the mineralisation, (ii) other alteration/metamorphic events in the host sequences, and (iii) aspects of alteration on a regional scale (Fig. 9).

## The deposits and their immediate environs

### *Osborne*

Osborne has a resource of ~12 Mt at ~3.0% Cu and 1.3 g $t^{-1}$ Au (Australian Register of Mining 1995/1996). The deposit is associated with silicification, and occurs in discordant lodes within metamorphosed rocks of the Soldiers Cap Group (Adshead 1996: EGRU, Contribution 55, 1–4). Samples representative of both pre-alteration metamorphic and hydrothermal alteration minerals were selected for $^{40}Ar/^{39}Ar$ dating. The following phases, from the eastern high-grade (ore) zone, were dated:

- actinolite (which is pre-ore and defines a metamorphic foliation) and biotite (which is associated with sulphides and cross-cuts the actinolite) from the massive pyrrhotite–chalcopyrite hangingwall zone; and
- hornblende (which is associated with biotite, magnetite, and Au-bearing chalcopyrite) from a silica-flooded breccia.

The metamorphic actinolite gave a minimum plateau age of ~1590 Ma; the hydrothermal biotite and hornblende each gave a plateau age of ~1540 Ma. The ~1590-Ma age is older than the ~1530-Ma age usually accepted for peak metamorphism according to age determinations in the western Mount Isa Inlier (e.g., Connors & Page 1995: Precambrian Research, 71, 131–153). On a district scale, sericite and muscovite from a granite ~10 km from Osborne each gave a plateau age of ~1465 Ma. Metamorphic biotite from a pelite at Osborne South had a maximum age of ~1568 Ma.

### *Ernest Henry*

The Ernest Henry deposit, ~40 km northeast of Cloncurry, has an indicated resource of 132 Mt at 1.1% Cu and 0.6 g $t^{-1}$ Au (Australian Register of Mining 1995/1996). The deposit, which is inferred to be syn- to post-late D3 deformation, occurs within a breccia system. The breccia system occupies a sequence of altered porphyritic intermediate volcanic rocks, and is bounded by shear zones associated with intense magnetite–biotite alteration (Craske 1995; AIG, Bulletin 16, 95–109). Alteration biotite associated with the mineralisation was selected for dating. The biotite, which forms part of a hydrothermal alteration assemblage that also contains magnetite and chalcopyrite, overprints a hematite-rich red-rock alteration product. It gave a plateau-like segment age of ~1478 Ma, which is considered to be contemporaneous with the Cu–Au mineralisation but younger than the intrusion of the nearby Naraku Batholith plutons (~1501 Ma, ~1505 Ma.).

### *Starra*

Starra is a stratabound Au–Cu deposit of 5.3 Mt at 5.0 g $t^{-1}$ Au and 1.98% Cu (Kary & Harley 1990: Australasian Institite of Mining & Metallurgy [AusIMM], Monograph 14, 955–963), and is hosted by a stratiform magnetite–hematite iron formation (Davidson 1992: op. cit.). It is represented by massive to banded quartz–magnetite–chalcopyrite–gold–scheelite-bearing ironstone, and subordinate quartz–chlorite–albite–magnetite schists in the footwall. It evinces extensive albite alteration overprinted by local potassium–iron alteration (biotite–magnetite), which evolved into magnetite-dominant alteration. Pyrite, chalcopyrite, calcite, and gold precipitated from later oxidising fluids that chloritised biotite and hematitised magnetite (Williams et al. 1995: AusIMM, Pac-Rim '95, 631–636). Alteration biotite spatially associated with chalcopyrite was selected for dating. It paragenetically predates the chalcopyrite, and overprints the banding in the ironstone. It has a plateau-like segment age of ~1503 Ma.

### *Mount Elliott*

The Mount Elliott deposit is a calcic Cu–Au skarn hosted by amphibolite-grade phyllite and siliceous siltstone of the Kuridala Formation. It has an indicated resource of 2.9 Mt averaging 4.5% Cu equivalent (McLean & Benjamin 1993: AIG, Bulletin, 13, 47–50). The massive skarn is a pink feldspar–hematite alteration product overprinted by clinopyroxene, or hornblende–biotite, scapolite, calcite, and magnetite. Chalcopyrite and pyrite are disseminated interstitially, and pyrrhotite occurs in the upper part of the skarn. Cu–Au mineralisation and the bulk of the hydrothermal alteration occurred late in the deformation history. Alteration biotite selected for dating is spatially associated with chalcopyrite, and overprints foliated siltstone adjacent to a massive cross-cutting actinolite–chalcopyrite–pyrite-bearing vein. The alteration biotite and mineralisation chalcopyrite may be broadly, paragenetically associated, and appear to have formed on the margins of the actinolite–chalcopyrite–pyrite vein. The alteration biotite, sampled from the foliated siltstone, gave a maximum age of ~1496 Ma.

## Alteration associated with the Williams Batholith

### *Hematitic breccias in the Wimberu Granite*

Coexisting sericite and K-feldspar were sampled from a hematitic granitic breccia associated with late felsic aplitic phases of the Wimberu Granite near Florence Bore, about 17 km north-northwest of Hampden (Fig. 9). The sericite gave a plateau-like segment $^{40}Ar/^{39}Ar$ age of ~1476 Ma; the K-feldspar gave a K–Ar age of ~1194 Ma. K-feldspar from a second breccia body nearby gave a K–Ar age of 1361 ± 11 Ma. The K-feldspar is anomalously young relative to both the $^{40}Ar/^{39}Ar$ age of the sericite and the 1508-Ma U–Pb zircon age of the host granite (Page & Sun 1996: op. cit.). The dated K-feldspar samples are typical for the eastern succession — hematitic, fractured, and perthitic — characteristics that may conspire to frustrate the determination of reliable $^{40}Ar/^{39}Ar$ alteration or crystallisation ages from the regionally ubiquitous K-feldspar-bearing alteration assemblages.

### *Albitite pipe in the Gilded Rose Breccia*

Muscovite from an albitite intrusive pipe just east of the Gilded Rose mine, and ~60 km south-southwest of Cloncurry, yielded a K–Ar age of 1488 ± 11 Ma, which broadly agrees with U–Pb zircon ages of ~1501–1505 Ma from the Naraku Batholith to the north (Page & Sun 1996: op. cit.).

## Conclusions

The project successfully applied the $^{40}Ar/^{39}Ar$ dating method to establishing that Cu–Au mineralisation in the Cloncurry district followed peak metamorphism. It also established that this dating method can be applied to rocks as old as the Palaeoproterozoic for dating regional metamorphic events, hydrothermal alteration, and mineralisation.

The results show that the Ernest Henry, Starra, and Mount Elliott deposits are broadly contemporaneous with or slightly post-date late phases within the Williams and Naraku Batholiths. Peak metamorphism at Osborne might have been ~1590 Ma, whereas hornblende and biotite which predated the mineralisation and postdated the regional foliation formed at ~1540 Ma.

The ubiquitous pink to red K-feldspars intimately associated with alteration throughout the Cloncurry district are unlikely to yield crystallisation or alteration ages by either the $^{40}Ar/^{39}Ar$ or K–Ar method.

## Acknowledgments

We thank Billiton Australia, North Exploration, MIM Exploration, Normandy Poseidon, Pancontinental Mining, Placer Pacific, RGC Exploration, and WMC for supporting this project. Keith Hannan, Steve Twyerould, Marie Heineman, Rob Hartley, Alex Meyer, Neil Adshead, and Chris Heinrich assisted with the sampling and/or provided samples.

# Depths of emplacement of Precambrian layered intrusions in the East Kimberley

*Alfonso Trudu*[1, 2] *& Dean Hoatson*[3]

**Geothermobarometric studies of reaction coronas between olivine and plagioclase, together with late magmatic alteration assemblages, in gabbroic rocks have helped to explain the spatial evolution of the Palaeoproterozoic layered mafic–ultramafic intrusions in the East Kimberley. These studies, conducted within the framework of the National Geoscience Mapping Accord Kimberley–Arunta project, have shown that the intrusions were emplaced into middle to upper crustal levels at pressures of 0.24 to 0.67 GPa* (about 8 to 24 km). Four types of coronas have been recognised. Each type appears to correlate with a particular group of layered intrusions. Emplacement depths for the intrusions generally increase northeastwards along the Halls Creek Orogen. This progression to deeper crustal levels is consistent with an increase in metamorphic grade of the country rocks (Tickalara Metamorphics) from greenschist to granulite facies and the more extensive development of migmatites.**

## Classification of East Kimberley layered mafic-ultramafic intrusions

The Palaeoproterozoic layered mafic–ultramafic intrusions in the East Kimberley (Fig. 10) have created considerable exploration interest for different styles of stratabound and hydrothermally remobilised platinum-group-element (PGE), Cr, Ni, Cu, Au, Ti, and V mineral deposits (Hoatson et al. 1995: AGSO Research Newsletter 22, 1–2). However, the different types of mafic–ultramafic intrusions and their depths of emplacement on a regional scale have remained unknown. On the basis of different metamorphic–structural histories, types of mineralisation, and high-precision U–Pb zircon geochronology, these intrusions can be assigned to seven major groups (I to VII; Fig. 10) that were emplaced between 1860 and 1830 Ma (Page et al. 1995: AGSO Research Newsletter 22, 7–8).

## Corona textures

Geothermobarometric studies by AGSO were carried out on 13 layered mafic–ultramafic intrusions representing groups I, II, III, V, and VI, namely: I — Big Ben, Panton; II — Springvale, Wilagee; III — Toby; V — Dave Hill, Keller Creek, McKenzie Spring, Sally Malay, Spring Creek, Wilson Creek; and VI — Armanda, McIntosh. Most of the rocks studied are mafic cumulates (olivine gabbronorite, troctolite, norite); the exceptions are a plagioclase peridotite (Big Ben) and a subophitic (non-cumulate) biotite ± quartz gabbronorite (Toby). The mafic cumulates consist mainly of cumulus olivine and cumulus plagioclase, whereas orthopyroxene and clinopyroxene, where present, tend to form intercumulus phases. Trace to minor minerals include apatite, biotite, chromite, magnetite–ilmenite, quartz, spinel, sulphides, and zircon.

The four types of coronas identified between olivine and plagioclase possibly represent progressive stages in the replacement of olivine from the least replaced (type 1) to the most replaced (type 4). Type 1 coronas in the Wilagee intrusion (group II) consist of extremely thin (up to 0.03 mm) symplectites, which are difficult to resolve optically into their individual components (probably amphibole and spinel) around subhedral olivine. Type 2 (Fig. 11) is the most common corona in the Dave Hill, Sally Malay (both group V) and McIntosh (group VI) intrusions, in which it surrounds partly embayed olivine grains. It consists of an inner rim (up to 0.02 mm) of orthopyroxene, and an outer zone (up to 0.3 mm) of green–brown amphibole grading outwards into a radiating symplectite of the same amphibole and small irregular rods of green–blue spinel. Type 3 coronas, as seen in the Keller Creek intrusion (group V), have a very thin (up to 0.015 mm) orthopyroxene rim that surrounds olivine and is partly overgrown by a much wider (up to 0.04 mm) zone of brown amphibole with embedded dark green spinel. In type 4 coronas, which are restricted to the plagioclase peridotite of the Big Ben intrusion (group I), olivine is rimmed by amphibole which grades outwards into a zone of coarser-grained blue–green spinel anhedra.

## Mineral chemistry

Cumulus, intercumulus, and corona mineral compositions for all intrusions, except Panton, were determined by the Cameca electron-microprobe at the Research School of Earth Sciences, Australian National University. Data for amphibole from the Panton intrusion were obtained from Hamlyn (1977: PhD thesis, University of Melbourne). Cumulus olivine analysed displays a similar wide range in *mg* number (40 to 83; *mg* number = atomic ratio Mg/[Mg+Fe], where Fe = total Fe) to that of cumulus, intercumulus, and corona orthopyroxene (49 to 81). There is a strong sympathetic correlation in *mg* number between olivine and the surrounding corona orthopyroxene. Most amphiboles analysed are Ca-rich (hornblende, tschermakite), but Fe–Mg amphibole (cummingtonite) is present in the Springvale and Spring Creek intrusions. Plagioclase is generally very calcic ($An_{70–98}$), but is more evolved ($An_{50–70}$) in the Keller Creek, Springvale, Toby, and Wilson Creek intrusions. The spinels in the coronas are hercynite and spinel, *sensu stricto*, with different $Mg/(Fe^{2+} + Mg)$ ratios of 45 to 65.

## Origin of coronas, and geothermobarometric results

A late magmatic rather than a metamorphic origin is favoured for the coronas because:

- orthopyroxene has the same *mg* number where it occurs as both an intercumulus and corona mineral;
- an apparent correlation between the type of corona and the different groups of intrusions indicates a local control influenced by composition or depth of emplacement rather than by (amphibolite-facies) regional metamorphism; and
- the textures of the coronas in the East Kimberley intrusions are similar to those of magmatic coronas described in overseas intrusions (Joesten 1986: Mineralogical Magazine, 50, 441–467; Acquafredda et al. 1992: Mineralogy and Petrology, 46, 229-238).

The Ti content of amphibole in the coronas was used to determine their temperature of formation (Otten 1984: Contributions to Mineralogy and Petrology, 86, 189–199), and the Al content of the same mineral was used for estimating pressure (Anderson & Smith 1995: American Mineralogist, 80, 549–559). In some samples where the coronas were poorly developed, or the Ti content of the clinoamphibole in the corona was too low (< ~0.1% $TiO_2$), the Ti content of late magmatic amphibole replacing clinopyroxene was used. Temperatures determined range from 665 to 800°C, which are similar to those documented (580 to 880°C) by Acquafredda et al. (op. cit.). Calculated crystallisation pressures range from 0.24 to 0.67 ± 0.06 GPa, which equate to middle to upper crustal depths of around 8 to 24 km, according to a gradient of 35 km $GPa^{-1}$ for 'normal' continental crust. Liquidus temperatures for the magmas are believed to be in the range of 1100 to 1300°C, which are similar to other mafic intrusions emplaced in the middle to upper crust (Hoatson et al. 1992: BMR [AGSO] Bulletin 242).

The pressures obtained are generally consistent within each group of intrusions, but differ between the groups. For example, the Cr–PGE–Ni–Cu-bearing Panton and Big Ben intrusions of group I have pressures of 0.32

[1] Consulting Geologists Australia Pty Ltd, 12 Hourigan Avenue, Clayton, Vic. 3168; tel. & fax +61 3 9543 4182.

[2] Department of Earth Sciences, Monash University, Clayton, Vic. 3168; tel +61 3 9905 4879; fax +61 3 9905 4903; e-mail esc158t@vaxc.cc.monash.edu.au.

[3] Minerals Division, Australian Geological Survey Organisation, GPO Box 378, Canberra, ACT 2601; tel +61 6 249 9593; fax +61 6 249 9983; e-mail dhoatson@agso.gov.au.

* 1 GPa = 10 kb.

and 0.31 GPa respectively. A lower pressure of 0.24 GPa for the group III Toby intrusion is consistent with the fine-grained subophitic texture and evolved mineralogy (apatite–biotite–magnetite–ilmenite–quartz–zircon) of the gabbros in this body. The Ni–Cu–Co-bearing intrusions of group V in the north cluster at the upper end of the pressure spectrum at 0.57 to 0.67 GPa. They also show well-developed coronas, which, according to Joesten (op. cit.), form at pressures in excess of 0.5 GPa. The different pressures for the McIntosh (0.5 GPa) and Armanda (0.28 GPa) intrusions of group VI can be rationalised if the relative stratigraphic levels of the samples are considered and if the Armanda intrusion correlates with the upper part of the McIntosh intrusion. The McIntosh sample is from near the base of a 7.8-km-thick body and the Armanda sample is from the middle of a 0.7-km-thick body.

R.G. Warren (formerly AGSO, personal communication 1995) has estimated emplacement pressures for the Sally Malay, McIntosh, and Springvale intrusions from high-temperature assemblages in contact metamorphic rocks. According to Fe/Mg partitioning between coexisting garnet and cordierite in metapelites adjacent to the Sally Malay and McIntosh intrusions, and the sta-

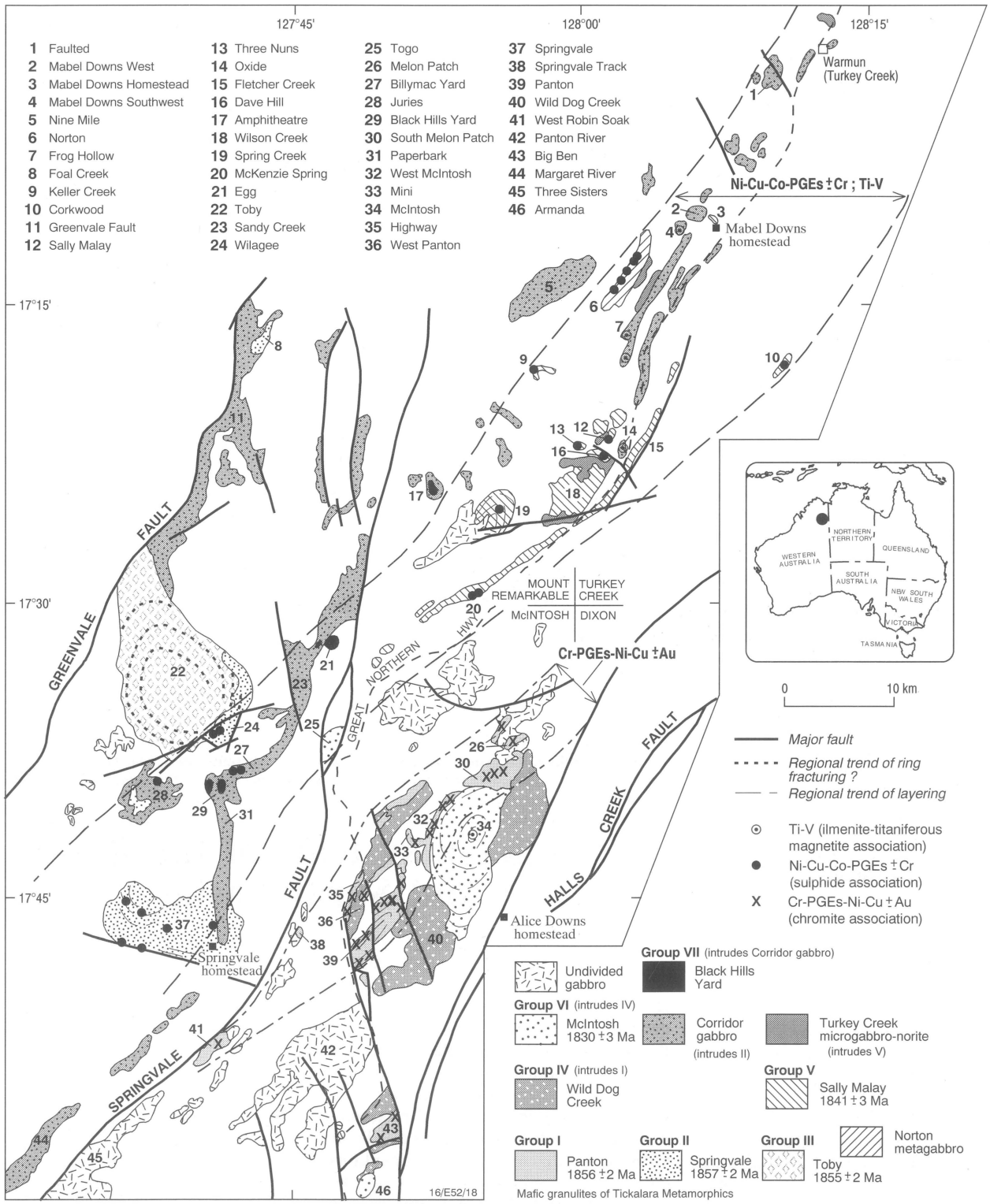


**Fig. 10. Regional distribution of Palaeoproterozoic layered mafic–ultramafic intrusions in the East Kimberley. The two northeast-trending parallel corridors containing mineralised intrusions are bounded by the dashed lines. Intrusions investigated in this study are: Keller Creek (9), Sally Malay (12), Dave Hill (16), Wilson Creek (18), Spring Creek (19), McKenzie Spring (20), Toby (22), Wilagee (24), McIntosh (34), Springvale (37), Panton (39), Big Ben (43), and Armanda (46).**

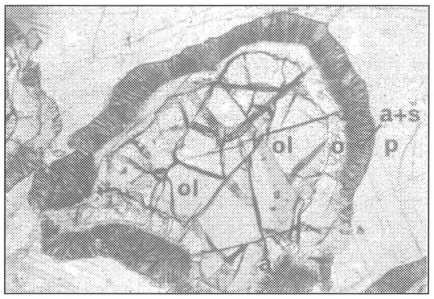


**Fig. 11. Photomicrograph of a type 2 corona from the Dave Hill mafic–ultramafic intrusion. ol = olivine; o = orthopyroxene; a = amphibole; a+s = amphibole and spinel symplectite, p = plagioclase. Sample 93522114, plane polarised light, field of view is 1.2 mm.**

bility of cordierite in a metasomatised raft in the Springvale intrusion, she estimated pressures of 0.4 to 0.5 GPa for Sally Malay, 0.5 to 0.6 GPa for McIntosh, and about 0.4 GPa for Springvale. These pressures are consistent with the results of this study.

## Some implications

The geothermobarometric results have important implications for the geological evolution of the East Kimberley, namely:

- estimated crystallisation pressures for the layered intrusions generally increase from less than 0.55 GPa in the southwest to greater than 0.55 GPa in the northeast of the study area (Fig. 12); these deeper crustal levels (i.e., deeper erosional levels) northeastwards along the Halls Creek Orogen are consistent with the increase in metamorphic grade of the country rocks (mainly Tickalara Metamorphics) from greenschist to granulite facies and the increased development of migmatites;
- the presence of chilled and contaminated margins, comagmatic satellite intrusions, and narrow (50-m) contact aureoles, and the correlation between depth of emplacement and group/age of intrusion, indicate that most of the East Kimberley intrusions have crystallised in situ and are not tectonically emplaced segments of larger bodies, as suggested by Hancock & Rutland (1984: Journal of Geodynamics, 1, 387–432);
- the crystallisation pressure of 0.32 GPa for the Panton intrusion is much lower than the 0.8 to 0.9 GPa (~30 km) proposed by Hamlyn (1980: American Journal of Science, 280, 631–668);
- the Ni–Cu–Co-bearing group V intrusions (e.g., Sally Malay) were emplaced at deeper crustal levels (20 to 24 km) than the Cr–PGE–Ni–Cu-bearing intrusions of group I (11 km: Panton); and
- similar pressures support the suggestion (Hoatson 1993: AGSO Research Newsletter 19, 9–10) that the Big Ben intrusion (0.31 GPa) is a transposed tectonic slice of the mineralised Panton intrusion (0.32 GPa) that has undergone a sinistral displacement of 15 km south along the Panton Fault.

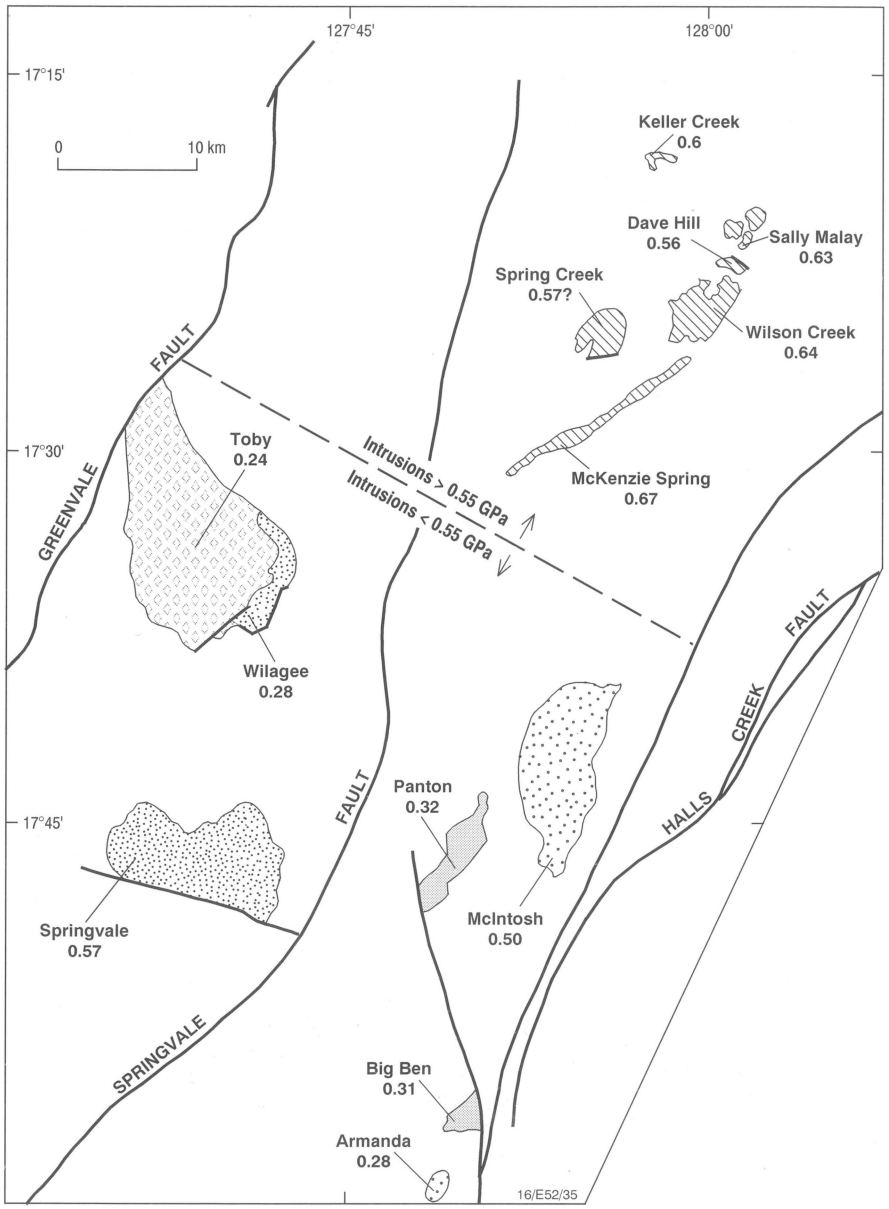


**Fig. 12. Calculated crystallisation pressures in gigapascals for the thirteen layered mafic–ultramafic intrusions studied. All estimated pressures have an uncertainty of ± 0.06 GPa. The end of the pointer for each intrusion indicates the approximate location of the sample(s). See Figure 10 for the key to symbols.**

# Petroleum systems of the Bowen and Surat Basins

*Russell J. Korsch[1], Chris J. Boreham[1], Tom S. Loutit[1], Jennie M. Totterdell[1], Malcolm G. Nicoll[1], & Ray D. Shaw[2]*

**Hydrocarbons were produced in great quantity in the central Bowen and Surat Basins according to the results of a recently completed petroleum resource evaluation. The bulk of them was generated after 140 Ma, mostly in the Early Cretaceous. As their estimated volume far exceeds the volume of discovered hydrocarbons (currently 45 million barrels of oil; 0.5 TCF of gas), controls on their preservation might be a significant risk factor. Even so, areas of maximum generation are located in discrete migration cells, and provide interesting insights into the prospectivity of large parts of the Bowen and Surat Basins, particularly the eastern margin.**

[1] Petroleum & Marine Division, Australian Geological Survey Organisation, GPO Box 378, Canberra, ACT 2601; tel. +61 6 249 9495 (RJK), +61 6 249 9488 (CJB), +61 6 249 9397 (TSL), +61 6 249 9407 (JMT), +61 6 249 9542 (MGN); fax +61 6 249 9972 (RJK, JMT, MGN), +61 6 249 9965 (TSL), +61 6 249 9983 (CJB); e-mail rkorsch@agso.gov.au, cboreham@agso.gov.au, tloutit@agso.gov.au, jtotterd@agso.gov.au, mnicoll@agso.gov.au.

[2] Vanibe Pty Ltd, 5A Mulbring Street, Mosman, NSW 2088; tel. and fax +61 2 9969 3223.

## Petroleum-oriented studies

The 'Sedimentary basins of eastern Australia' (SBEA) National Geoscience Mapping Accord (NGMA) project is scheduled for completion at the end of 1996. This project — a joint venture between AGSO, the Geological Survey of Queensland, and the Geological Survey of New South Wales — was conceived as a regional study of the Bowen, Gunnedah, and Surat Basins, and was designed to improve our understanding of the effect of geological processes on resource systems. Project investigations focused particularly on province and terrane analysis, regional and basin analysis, play-element evaluation, and, in more detail, play-element evaluation and petroleum-systems definition in the central Bowen Basin.

Much of the work entailed structural and sequence stratigraphic mapping of a regional grid defined by seismic data acquisition. This aspect of the work defined the stratal geometry of the sedimentary units through time, and detailed the interplate and intraplate tectonic events that helped to create the accommodation space. As a result, for the central Bowen and northern Surat Basins, we have:

- defined the shapes of the basins within which organic-rich rocks (ORRs) have been deposited, and the character and timing of deposition of each ORR;
- determined the timing of hydrocarbon generation and the products generated;
- identified potential migration paths; and
- documented the timing and distribution of sequences containing seal and reservoir rocks.

The results of burial and maturation history modelling of 46 wells in the southern Taroom Trough show that maximum heat flow occurred at about 95 Ma, in the early Late Cretaceous. Over most of the study area in southern Queensland, the timing of

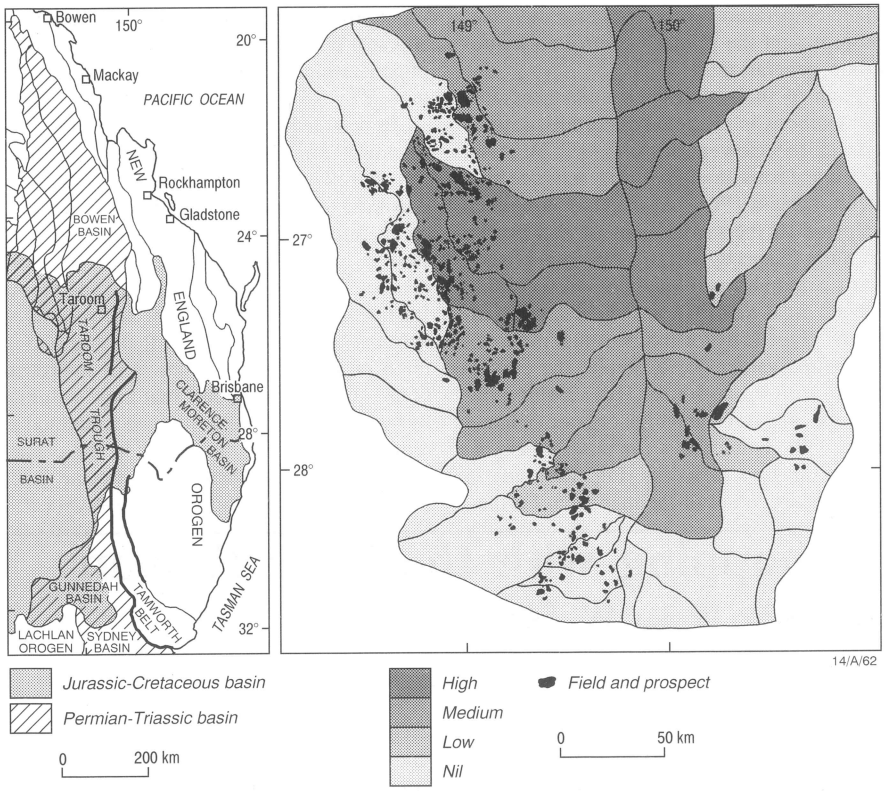


**Fig. 13. Relative oil yield per drainage cell, and the fields and a number of prospects, in the central Bowen Basin (from Shaw 1996).**

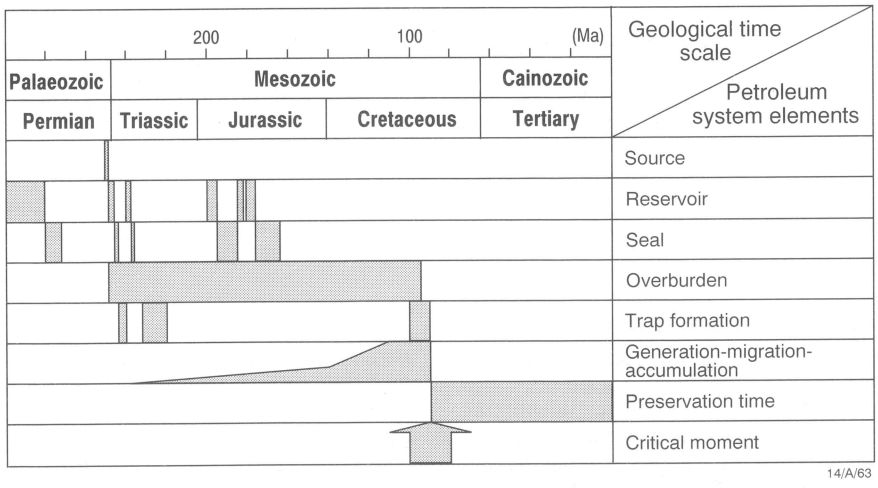


**Fig. 14. The Baralaba petroleum system in the central Bowen and northern Surat Basins in Queensland.**

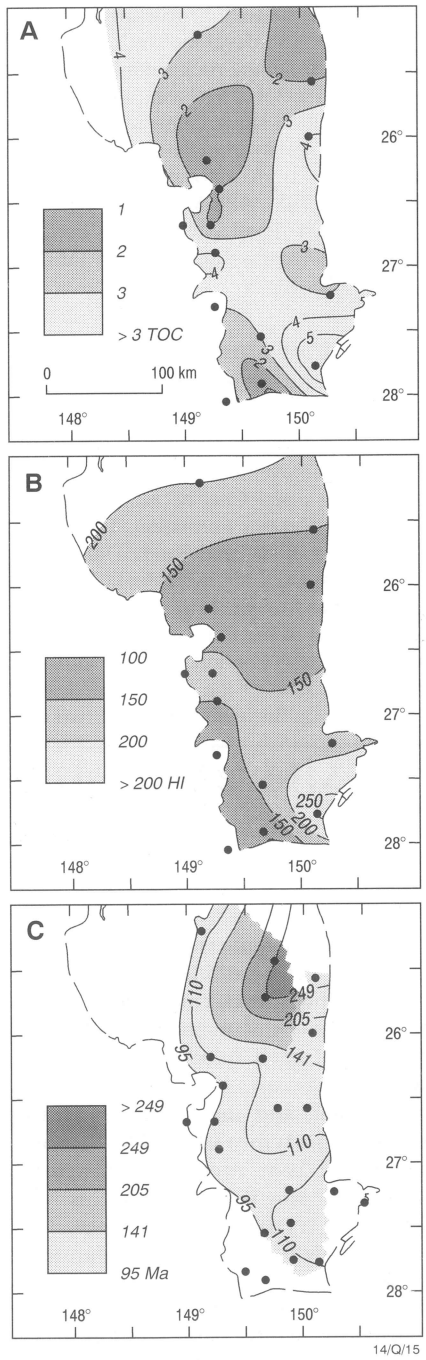


**Fig. 15. Regional maps of the Burunga mudrock petroleum system: a) average total organic carbon (TOC) content; b) average initial hydrogen index (HI); c) age (Ma) when the top of the Burunga Formation reached TR = 0.1 (transformation ratio; TR = 0.1 is considered to represent the onset of oil generation and primary migration). All contours are confined to within the limits of the B60 sequence boundary (base of upper Burunga Formation, which is represented by the dashed line).**

the main phase of hydrocarbon generation and expulsion coincided with increased heat flow and possibly extension in the Early Cretaceous. Although various sedimentary successions throughout the southern Taroom Trough undoubtedly reached maturity, the quantity and quality of the organic matter would have determined whether the resulting hydrocarbons were adequate to support primary migration from the source rock.

From an extensive geochemical database which the project developed for hydrocarbon and potential source-rock samples from the Queensland sector of the basin, an oil–source-rock correlation study confirmed a Permian source for the hydrocarbons, and a minor contribution from a local Triassic source (Boreham 1995: APEA, Journal 35, 579–612). A much smaller database is currently being compiled for samples from the New South Wales sector.

## Outcome of studies: the Bowen Basin as an example

The project has documented six effective source-rock units in the Bowen Basin: the Triassic Moolayember Formation, and the Permian Baralaba Coal Measures, Burunga Formation, Banana Formation, Flat Top to Buffel Formations, and Reids Dome beds. We have assessed the individual oil and gas contributions from coal and mudrock in them. Source rocks in the Baralaba Coal Measures and the Burunga Formation have contributed over 90 per cent of the oil generated in the central Bowen Basin, and the same two units plus the Flat Top to Buffel and the Banana Formations have contributed about 90 per cent of the gas.

The combination of high heat flow and extra sediment thickness during the Early Cretaceous accounted for most of the hydrocarbon generation, and induced the bulk of the Permian source rocks to expel oil and gas for the first time. Only in those parts of the basin where the sediment pile was thickest (particularly along the axis of the Taroom Trough) were hydrocarbons generated earlier, starting in the Late Permian but mainly during the Triassic. On the western margins of the basins in Queensland, major trap formation probably coincided with the high rate of hydrocarbon generation and expulsion in the Early Cretaceous. Maximum palaeotemperatures were evident at this time, and represent the primary control on hydrocarbon generation.

Each of the source-rock units generated hydrocarbons in discrete structurally defined parts of the Bowen Basin (Fig. 13). Also, each one forms the basis of a separate petroleum system (Fig. 14) that has now been evaluated in the central part of the Bowen and Surat Basins by Shaw (1996: unpublished report commissioned by AGSO). According to TOC areal distribution (Fig. 15a) and initial HI (Fig. 15b) for the Burunga mudrock petroleum system, for example, the combination of oil-prone source (HI >200 mg hydrocarbons/g TOC) and high organic richness (TOC >3%) would have favoured oil expulsion during the Cretaceous (Fig. 15c) only in the southeast corner of the map area. Further, this petroleum system was the main contributor to the oil generated in the south.

## Regional implications

Our estimates of the timing and products of generation, and of the relative yields of the more effective ORRs, offer insights into the potential for new plays in the region. We consider that the present-day structure is a reasonable representation of the geometry of the central Bowen Basin at the time of generation during the Early Cretaceous. Thus the distribution and character of reservoir and seal units and traps can be overlaid on potential migration pathways from the centre of the basin, particularly at the relatively unexplored eastern margin of the basin. The timing of the emplacement of trap, reservoir, and seal play elements relative to the timing of generation is documented on timing charts (e.g., Fig. 14).

In conclusion, the SBEA project has produced a consistent tectonostratigraphic framework over a large region of eastern Australia that will form the basis for regional evaluation of the petroleum systems in the Bowen, Surat, and Gunnedah Basins. A more detailed study of the central Bowen and Surat Basins suggests that at least six petroleum systems operated there, but that only two or three produced large volumes of hydrocarbons. The results suggest that large volumes of hydrocarbons might have accumulated in a number of unexplored areas in the central Bowen and Surat Basins, but offer no clues about the potential for their preservation.

# Alteration mineral mapping with the laser Raman microprobe: a new technique

*Terrence P. Mernagh[1], Kenneth C. Lawrie[1], & Julienne Kamprad[1]*

**The laser Raman microprobe offers a new and rapid method of identifying minerals in thin sections, rock chips, and drillcore. Advantages of this method include visual selection of each mineral, spot analysis (down to 1 μm), little or no sample preparation, and the ability to identify mineral polymorphs. The Raman technique is a form of vibrational molecular spectroscopy that is very sensitive to crystal structure; hence, it can be used to identify a wide range of minerals — including most silicates, carbonates, sulphates, nitrates, phosphates, hydroxides, oxides, and sulphides. The small spot size also makes this a powerful method for the identification of very fine-grained mixtures of minerals, such as those commonly encountered in alteration zones surrounding hydrothermal mineral deposits.**

Many alteration haloes show a zonation of mineral assemblages resulting from the changing composition of the hydrothermal fluid as it flowed through the host rocks. Alteration may vary from minor colour changes to extensive mineralogical transformations and complete recrystallisation. Correct identification of both the primary and altered mineral assemblages is necessary for a proper understanding of the ore-forming processes and exploration for similar styles of deposits. Often, geologists must rely on their powers of observation or simple tests (e.g., staining) to identify minerals in drillcore or hand specimens, but if these are inconclusive then more detailed laboratory procedures are required. However, the need for time-consuming sample preparation can now be obviated, as the laser Raman microprobe (Fig. 16) provides a rapid, non-destructive analysis at the micron scale of any specimen which can be placed under a microscope.

## Examples of alteration styles

### *Porphyry Cu–Au mineralisation*

In the porphyry environment, identifying mineral assemblages helps establish the relative locations of samples within the hydrothermal system. Establishing these criteria facilitates both the recognition of fluid pathways and, ultimately, the determination of vectors to mineralisation. However, the very fine grainsize of many of the constituent minerals in these alteration assemblages can make them difficult to identify in hand specimen. Also, discrimination between alteration styles is commonly a severe problem in more oxidised systems where hematitic dusting can impart a pink colour to the feldspar alteration; this makes it difficult to discriminate between alteration containing only hematite and that with hematite-dusted feldspar (sodic or potassic).

Traditionally, identification of these fine-grained alteration assemblages has relied on a combination of thin section, X-ray diffraction (XRD) and staining techniques, and, more recently, PIMA* spectral data. Even

[1] Minerals Division, Australian Geological Survey Organisation, GPO Box 378, Canberra, ACT, 2601; tel. +61 6 249 9640 (TPM), +61 6 249 9847 (KCL), +61 6 249 9274 (JK); fax +61 6 249 9983; e-mail tmernagh@agso.gov.au, klawrie@agso.gov.au, jkamprad@agso.gov.au.

* Portable Infrared Mineral Analyser (an infrared reflectance spectrometer). Note that the use of brand names does not represent an endorsement of these products by AGSO.

**Fig. 16. Dr Terry Mernagh analysing a sample of rock with AGSO's Microdil 28 laser Raman microprobe.**

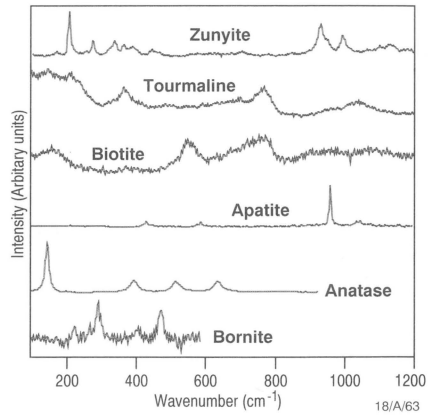


**Fig. 17. Laser Raman microprobe spectra of minerals which may occur in alteration assemblages of porphyry Cu–Au deposits.**

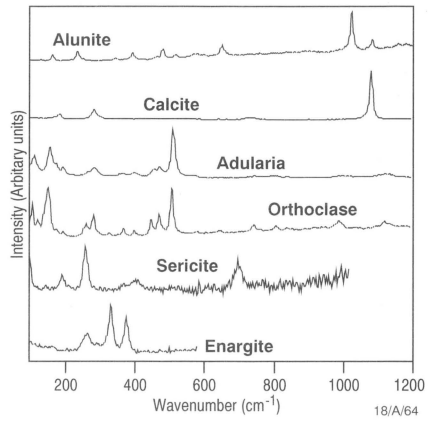


**Fig. 18. Laser Raman microprobe spectra of minerals which may occur in alteration assemblages of epithermal deposits.**

with these specialised techniques, the constituents of an assemblage are often difficult to uniquely identify owing to the mixing of the minerals at the microscope scale.

The laser Raman microprobe can provide more definitive data for resolving the constituents of such assemblages. Thus, albitic, potassic, and hematitic alteration styles, which may appear very similar in hand specimen, yield distinctive Raman spectra. Dark or opaque minerals (e.g., tourmaline, biotite, and bornite) tend to give weak but distinct spectra which still allow their proper identification.

Another advantage of Raman spectroscopy is that it can easily identify the various $TiO_2$ and other polymorphs. For example, anatase (Fig. 17) gives a very intense Raman spectrum, allowing even minute crystals to be readily detected. Preliminary studies of some Ordovician porphyry Cu–Au occurrences from New South Wales indicate that anatase and brookite are present in biotite alteration assemblages, in which these $TiO_2$ phases previously had been identified as rutile. Anatase is an indicator of low temperatures and possibly low fluid pH (Mathews 1976: American Mineralogist, 61, 419–424). We are now investigating how these $TiO_2$ polymorphs relate to depth of formation and to differences between high and low sulphur systems. The potential use of $TiO_2$ phases as indicators of porphyry environments is also currently being examined in resistate mineral studies (K. Scott, CSIRO Division of Exploration & Mining, personal communication 1996).

The laser Raman microprobe also facilitates rapid identification of more unusual minerals, such as zunyite (Fig. 17), which are characteristic of low-sulphur high-chlorine porphyry environments. The technique could be of particular importance in skarn environments where rapid identification of key accessory/indicator minerals is possible.

### *Epithermal mineralisation*

Many minerals can be quickly identified by noting the frequency of the most intense band in the Raman spectrum. For example, most sulphates display an intense band near 1000 $cm^{-1}$; carbonates have an intense band near 1100 $cm^{-1}$; and feldspars have an intense band near 510 $cm^{-1}$. For other minerals, more than one band may be needed. Hence, sericite is characterised by bands near 100, 265, and 700 $cm^{-1}$, and the characteristic bands for sulphides occur below 500 $cm^{-1}$.

The identification of adularia is critical for distinguishing low-sulphidation systems; this mineral is one of the indicators of boiling. Since all adularia types have compositions close to pure orthoclase, the mineral is extremely difficult to identify by other analytical techniques (Dong & Morrison 1995: Mineralium Deposita, 30, 11–19). However, the structural disorder commonly present in adularia is reflected in its Raman spectrum, which has fewer peaks and broader bands than that of orthoclase (Fig. 18). Thus, Raman spectroscopy is a useful method for distinguishing between these two minerals, especially when the distinctive morphology of adularia is difficult to recognise.

Similarly, the laser Raman microprobe can also distinguish the various silica polymorphs (Kingma & Hemley 1994: American Mineralogist, 79, 269–273), making it potentially useful for determining the structural level of preservation of epithermal vein systems. Its ability to obtain spectra of both crystalline and non-crystalline materials might facilitate the recognition of thermal overprinting of veins in which the textures of epithermal and low-temperature quartz are visually preserved but the minerals are actually recrystallised.

Raman spectroscopy may be particularly useful in high-sulphidation epithermal systems, in which the friable and vuggy alteration assemblages near a mineral deposit preclude the preparation of good-quality thin sections. The laser Raman microprobe also provides a useful method for discriminating between key sulphide minerals (Mernagh & Trudu 1993: Chemical Geology, 103, 113–127), such as luzonite and enargite (Fig. 18), which are commonly zoned within these systems. Their identification would otherwise require the preparation of systematic polished thin-sections and/or geochemical analysis.

## Comparisons with other techniques

In common with other spectroscopic techniques, Raman spectroscopy produces a spectral 'fingerprint' which can be used to identify each mineral. However, since it is a visible-light technique, fluorescent minerals or impurities in minerals may cause interference by producing sufficient fluorescence to swamp the weaker Raman signal. Using either a laser with a different wavelength or the complementary technique of infrared spectroscopy (the method used by the PIMA instruments) will generally overcome this problem. For example, PIMA can readily identify a number of clays which have strong fluorescence backgrounds in their Raman spectra. Be that as it may, PIMA does have its restrictions: it can detect only those minerals that contain water or OH and/or $CO_3$ groups, whereas the Raman microprobe can

identify a much larger range of minerals.

In theory, Raman spectra are similar to the infrared spectra produced by PIMA instruments, but the Raman bands are usually much sharper. The sharper Raman bands reduce the problem of overlapping bands (common in infrared spectroscopy) and make identification much easier. Both the Raman and PIMA instruments require little or no sample preparation and provide a rapid spectral analysis.

PIMA has the advantage of being portable and available for field use, whereas portable Raman spectrometers are still awaiting development. However, PIMA is designed to analyse a sample area of ~1 cm in diameter, which usually results in complex spectra representing mixtures of minerals; by contrast, the high spatial resolution (down to 1 μm) of the Raman microprobe allows each mineral to be identified separately.

The laser Raman microprobe is akin to a coarse sampling microprobe, but does not require a vacuum or a carbon-coated sample. Its ability to identify minerals *in situ* avoids the time-consuming sample preparation procedures associated with the preparation of thin sections or with analysis by X-ray fluorescence, X-ray diffraction, etc. Furthermore, X-ray methods may not detect minerals present in trace concentrations, but these may be readily identified using the Raman microprobe spot-analysis technique. Therefore, the laser Raman microprobe promises to be a very useful technique for the identification of minerals, not only in alteration assemblages but in samples from a wide variety of geological environments.

## Acknowledgment

We thank the Museum of Victoria for supplying a certified sample of zunyite.

# Complex attributes: new tools for enhancing aeromagnetic data

*Peter J. Gunn[1], Desmond Fitzgerald[2], & Nabeel Yassi[2]*

**We have applied complex algebraic theory to develop several new methods for presenting aeromagnetic data. This note discusses the theory and possible applications of our 'complex attributes'.**

The following mathematical description, which has been adapted from Taner et al. (1979: Geophysics, 44, 1041–1063), outlines how complex variable theory relates to profiles of magnetic (or any other) data.

A magnetic anomaly m(x) can be considered as the real part of a complex signal; thus:

$$M(x) = m(x) + j\, m^{*}(x)$$

where $m^{*}(x)$ is the imaginary (quadrature) component and M(x) is the complex signal, which is known as the analytic signal (cf. Roest et al. 1992: Geophysics, 57, 116–125).

$$|M(x)| = A(x) = [(m(x))^2 + (j\, m^{*}(x))^2]^{1/2}$$

where A(x) is the energy envelope which is the commonly used parameter in presentations of analytic signals in potential-fields studies.

$$\Phi(x) = \tan^{-1} [m^{*}(x)/ m(x)]$$

where $\Phi(x)$ is called the instantaneous phase.

$$d\Phi(x)/dx = \omega(x)$$

where $\omega(x)$ is the instantaneous frequency.

Taner et al. described a convolution approach of using a Hilbert transform to calculate the quadrature component for profile data.

## The complex attributes

The following examples of complex attributes are presented for profile data. Our reason for not initially using gridded aeromagnetic data is that profile aeromagnetic data has a much finer sample interval, and, as such, the results are not likely to be affected by problems caused by aliasing and interpolation. In previous studies in which we have calculated analytic signals, we have found that such effects can degrade the results for data sets in which the widths of anomalies are small relative to the flight-line spacing. We have selected a data set in which most of the magnetic features trend perpendicular to the flight lines, so that processing the profiles is likely to give results closely approximating a grid-based approach. Figure 19 presents our results.

We selected as our test data set (Fig. 19a) aeromagnetic data acquired on east–west flight lines spaced at 100 m and flown at a ground clearance of 60 m over the Broken Hill area of Australia. The sampling interval of the recording system was 7 m. The data were gridded to 20-m cells for display purposes, and presented as a straightforward image in which colour corresponds directly to amplitude. No sun-angle enhancement has been applied, although this would have increased the apparent detail in the data.

A **quadrature image** (Fig. 19b) of the same data set appears to show more detail than the original total magnetic intensity (TMI) image, perhaps because the quadrature data represent a 90° phase shift of the original

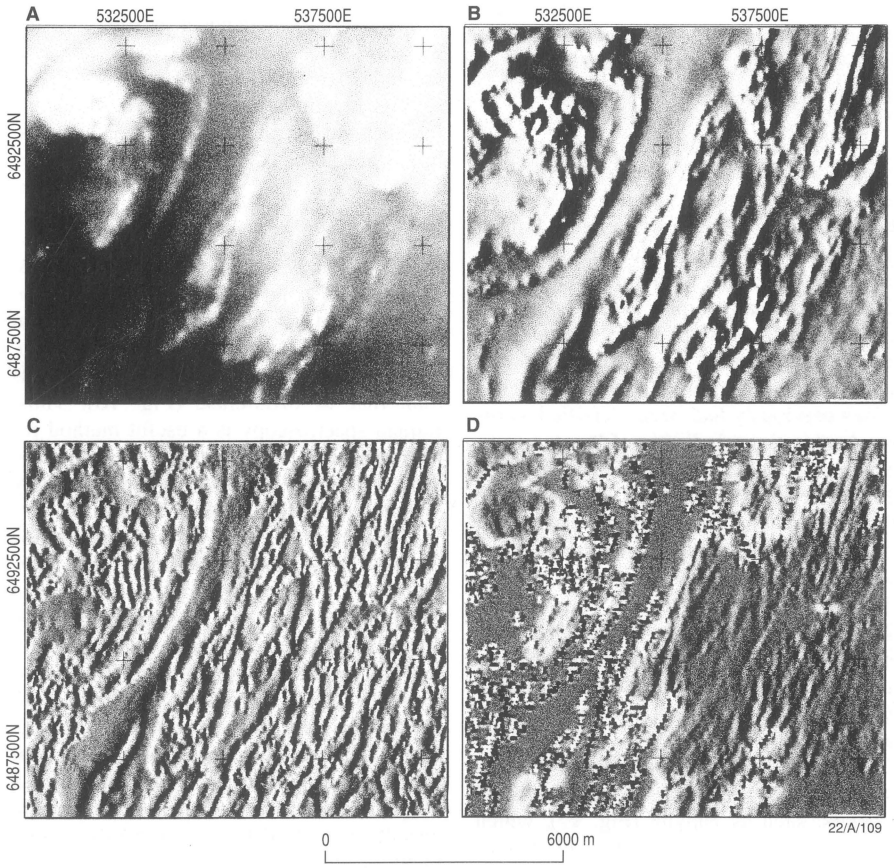


**Fig. 19. Examples of images of complex attributes applied to a component of the magnetic field over the Broken Hill area. (A) Total magnetic intensity. (B) The quadrature (imaginary) field. (C) The instantaneous phase, which maps anomaly continuity and accurately locates magnetic sources. (D) The instantaneous frequency, which maps anomaly character.**

1 Minerals Division, Australian Geological Survey Organisation, GPO Box 378, Canberra, ACT 2601; tel. +61 6 249 9226; fax +61 6 249 9986; e-mail pgunn@agso.gov.au.

2 Desmond Fitzgerald and Associates Pty Ltd, 2/1 Male St., Brighton, Victoria, 3186; tel. +61 3 9593 1077; fax +61 3 9592 4142.

data. This means that single-peak anomalies in the original TMI data become combinations of peaks and troughs in the quadrature data, and thereby become more obvious. This doubling of the number of anomalies assists the resolution of discontinuities. The position of the magnetic sources is expected to align more or less with the cross-overs from the positive to the negative parts of the quadrature anomalies for near-vertical north-striking magnetic sources. Our initial impression is that quadrature images could provide a valuable complement to TMI images.

The instantaneous phase of data has the property of emphasising the continuity of features, regardless of their amplitude values (Taner et al. 1979: op. cit.). Its value has been recognised in this respect in the processing of seismic data.

An **image of the instantaneous phase** (Fig. 19c) of our test data set suggests that it has a similar application in the processing of magnetic data. We believe that instantaneous phase has an advantage over automatic gain control (AGC), a technique commonly applied to mapping magnetic anomalies, for the following reasons (although we have not directly compared the two):

- small anomalies on the flanks of large anomalies can be almost eliminated in AGC processing; and;
- AGC can emphasise noise as well as continuity.

First and second vertical derivatives are often used to resolve the interfering magnetic effects of closely spaced magnetic sources. Comparisons of these derivatives processed for the data set of Figure 19a suggest that the instantaneous phase may have superior resolution qualities.

Taner et al. reported that the instantaneous frequency attribute can map character changes in seismic responses, and that some character changes, not obvious in conventional seismic data, have been found to correspond to gas accumulations. We therefore expect instantaneous frequency to evince character changes in magnetic data.

The **image of instantaneous frequency** (Fig. 19d) maps markedly different responses for areas which in the original TMI image (Fig. 19a) have little apparent difference in terms of magnetic response. At this stage of our investigations we have not ascertained exactly what factors control the changes in character being mapped by the instantaneous frequency. This process perhaps could be used to identify character changes due to mineralising processes.

## Acknowledgment

The results presented in this note were produced as a result of the MAGMAGE project, an ongoing collaborative project investigating new methods for processing and presenting airborne geophysical data. The MAGMAGE project is managed by AGSO in association with Desmond Fitzgerald and Associates Pty Ltd on behalf of a consortium of industry sponsors.

# Crustal architecture in northwest Tasmania revealed by deep seismic reflection profiling

*Barry J. Drummond[1], Russell J. Korsch[1], Tim J. Barton[1], & Tony (A.V.) Brown[2]*

**The results from two deep seismic reflection profiles recorded onshore in northwest Tasmania reveal for the first time the crustal architecture underlying Palaeozoic and Proterozoic elements in northwest Tasmania — including the Tyennan region, interpreted as the core of Tasmania. These profiles are among a comprehensive array of deep seismic lines that AGSO and the Geological Survey of Tasmania recorded both onshore and offshore as part of the multidisciplinary 'TASGO' National Geoscience Mapping Accord project. The primary objective of this project is to provide a regional tectonic framework for the State, for which geophysical data are providing the key controls on geological modelling at depth. The deep seismic profiles cross all major geological boundaries there.**

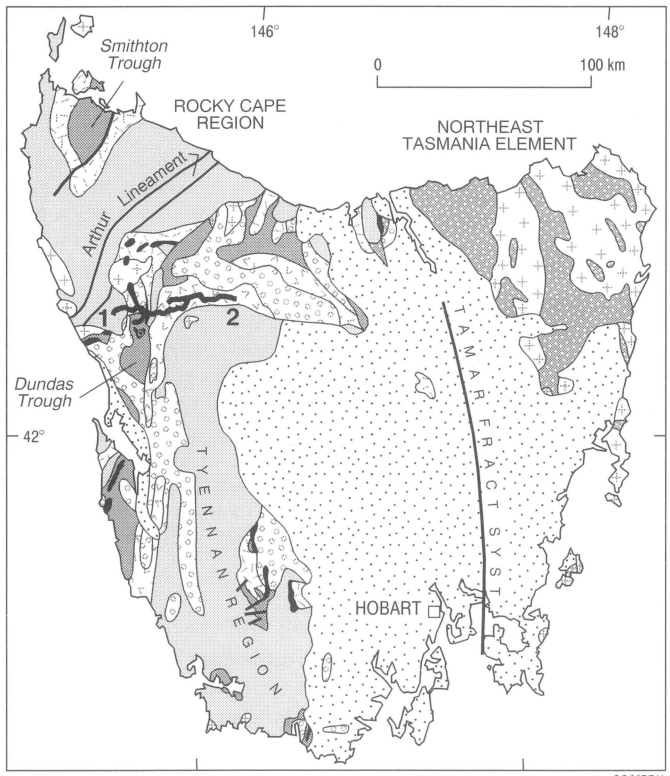


## Profile locations, and main features traversed

The two profiles whose results are presented here were both oriented roughly east–west along public roads (Fig. 20). Line 1 was positioned to begin as far west as practicable on the Proterozoic Oonah Formation, which crops out east of the Arthur Lineament, and then to profile as far east as access would allow. It crossed the highly mineralised Dundas Trough and Mount Read Volcanics outcrop before terminating at the Henty Fault Zone. Line 2 was offset about 15 km to the north of line 1, and started west of the Henty Fault Zone; that is, it overlapped the geological section covered by line 1, and continued east, approaching the Tyennan region obliquely from the north.

The Moho in northwest Tasmania appears as a transition zone, over 5 km thick (Fig. 21), in which strong lower crustal reflectors give way to a non-reflective mantle. The top of the transition zone is about 30–33 km deep (11–14 s two-way-time). The crust is partitioned into several distinct blocks. The most distinctive reflections, which dip at about 30° to the east, are attributed to

**Fig. 20. Onshore geology of Tasmania, and the locations of seismic lines 1 and 2 in the northwest.**

1 Petroleum & Marine Division, Australian Geological Survey Organisation, GPO Box 378, Canberra, ACT 2601; tel. +61 6 249 9381 (BJD), +61 6 249 9495 (RJK), +61 6 249 9760 (TJB); fax +61 6 249 9972; e-mail bdrummon@agso.gov.au, rkorsch@agso.gov.au, tbarton@agso.gov.au.

2 Geological Survey of Tasmania, PO Box 56, Rosny Park, Tasmania 7018; tel. +61 3 6233 8365, fax +61 3 6233 8338; e-mail tbrown@mrt.tas.gov.au.

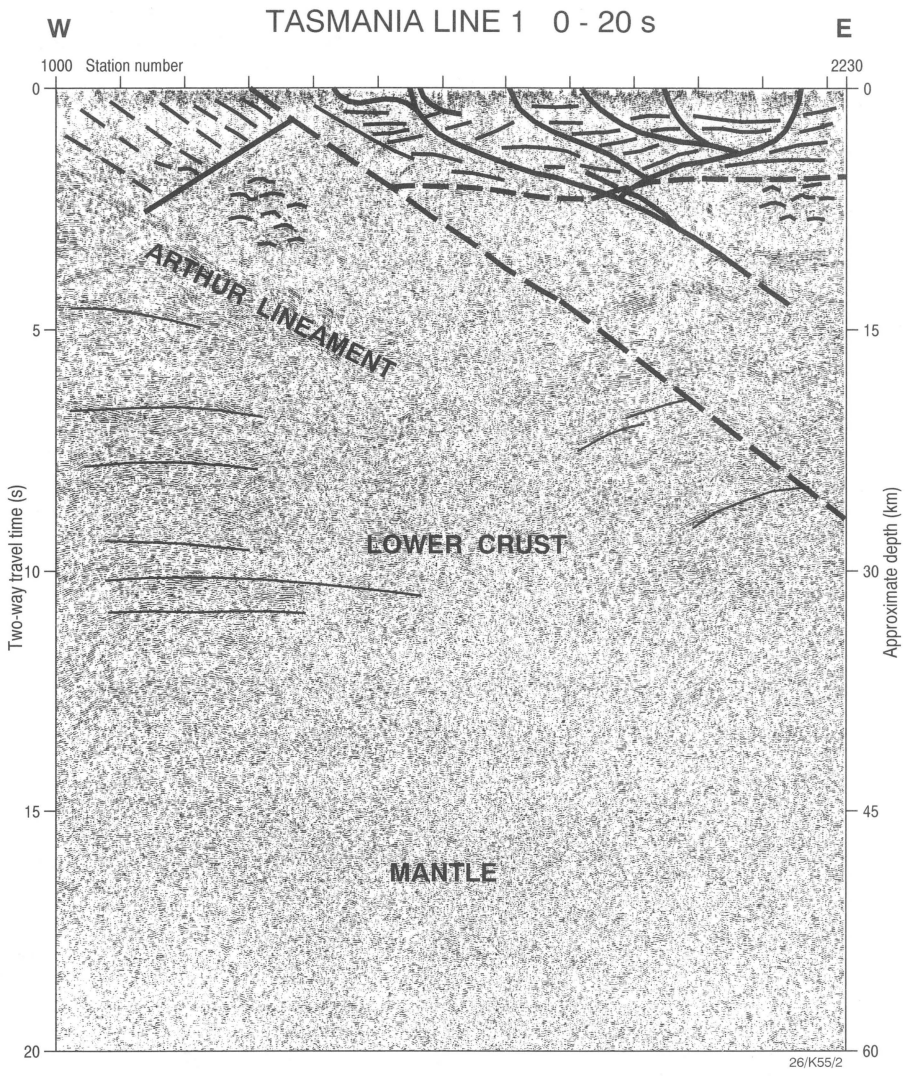


**Fig. 21. Crustal architecture along line 1. The vertical axis on the left shows the time taken for seismic energy to penetrate the Earth and reflect to the surface. The axis on the right has been converted to approximate depth. (V/H = 1 for a seismic velocity of 6 km $s^{-1}$).**

the Arthur Lineament, a major crustal feature underlying not only the rocks of the Oonah Formation and Dundas Trough but probably also at least the western part of the Tyennan region (Fig. 22).

## Precambrian rocks, prominent fault splays, and the Arthur Lineament

Neither seismic line reached outcrop of the Tyennan region. The eastern end of line 1 (Fig. 22) and line 2 (Fig. 23) display a consistent seismic reflection pattern of a very reflective lower crust, labelled as basement to the Tyennan region, which extends upwards to within about 10 km of the surface. This basement is overlain by several kilometres of rocks which are poorly reflective, interpreted to be the monotonous, mainly quartz-rich lithologies found in the Tyennan region. They, in turn, are overlain by more reflective rocks of the lower Palaeozoic section.

The boundary between the Tyennan region and basement appears to dip gently to the west in the west (Figs. 22–23). On the eastern side of line 1 (Fig. 22), a major fault system extends upwards to the west from within the Tyennan basement. Some splays off this system have associated outcrops of serpentinite (Fig. 22). Other major fault systems are also linked to this deep structure. The Henty Fault Zone, for example, dips west from the surface and meets it at a depth of about 7–8 km. The Rosebery Fault and several other unnamed faults link into a detachment which intersects the Henty Fault Zone at a depth of 3 km. These fault systems are close to volcanic-hosted massive sulphide deposits; the interpretation of the seismic data therefore suggests that crustal-scale tectonics have controlled the location of mineral deposits in northwest Tasmania.

Reflections from within the Oonah Formation in the west are parallel to the Arthur Lineament. Therefore, the boundary between the Oonah Formation and the Arthur Lineament can be interpreted equally as a conformable or unconformable stratigraphic contact, or a structural boundary (Fig. 22). At a depth of about 8 km, however, the overlying Oonah Formation is terminated abruptly by a west-dipping structure which extends upwards to the east. In the area of the seismic section, this structure does not crop out because it terminates against a major linear feature which dips eastwards, parallel to the Arthur Lineament, and forms the western edge of the Palaeozoic section.

## The Palaeozoic section and its partial Tertiary basalt cover

The Cambrian section in the Dundas Trough, and the Mount Read Volcanics, have a cumulative thickness which varies from less than 2 km in the east (near the eastern end of line 2, Fig. 23) to about 6 km in the west between shot points 1400 and 1600 on line 1 (Fig. 22). The seismic data suggest that the thickening to the west is stratigraphic rather than tectonic. Even so, the rocks are clearly highly folded and faulted, and the reflectivity of the data varies; the Mount Read Volcanics, for example, are poorly reflective, and their thickness shown in Figures 22 and 23 is to some extent interpretative.

The Ordovician to Lower Devonian section on line 2 is about 3 km thick (Fig. 23). This may not be representative of the true stratigraphic thickness, because the seismic data evince shortening on a series of thrust-ramps under Tertiary basalt (Tb) east of the Henty Fault Zone and north of the Tyennan region (between stations 2200 and 2400).

## Buried granites

Line 2 crosses several low gravity anomalies. Away from line 2, the edges of some of these anomalies coincide with outcropping granites. For this reason, two zones with no reflections in the seismic section along line 2 are interpreted as buried granites (Fig. 23). Each has about the same width:depth ratio. The granite at the eastern end of the line has a clearly imaged underside to the east, and is shaped like a drooping inverted tear-drop. The underside to the granite in the middle of line 2 is not imaged successfully. It appears to have an apophysis which extends to within several hundred metres of the surface. The apophysis also has an inverted tear-drop shape.

## Concluding observations and acknowledgments

In summary, onshore deep seismic reflection profiling in northwest Tasmania has provided images of the continental crust which show that the Palaeozoic section is cut by a set of linked major faults. The Arthur Lineament is a major, east-dipping crustal feature.

The foregoing interpretation has benefited greatly from discussions with David Leaman (consultant), and staff of the Geological Survey of Tasmania.

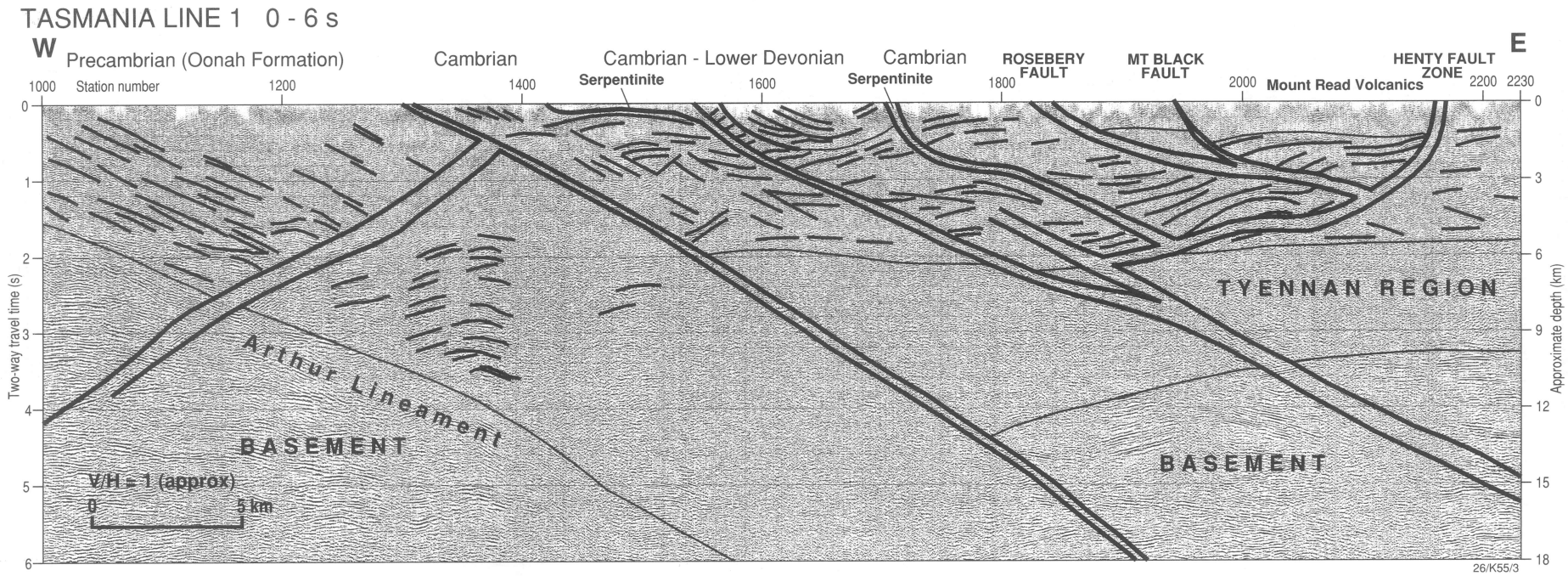


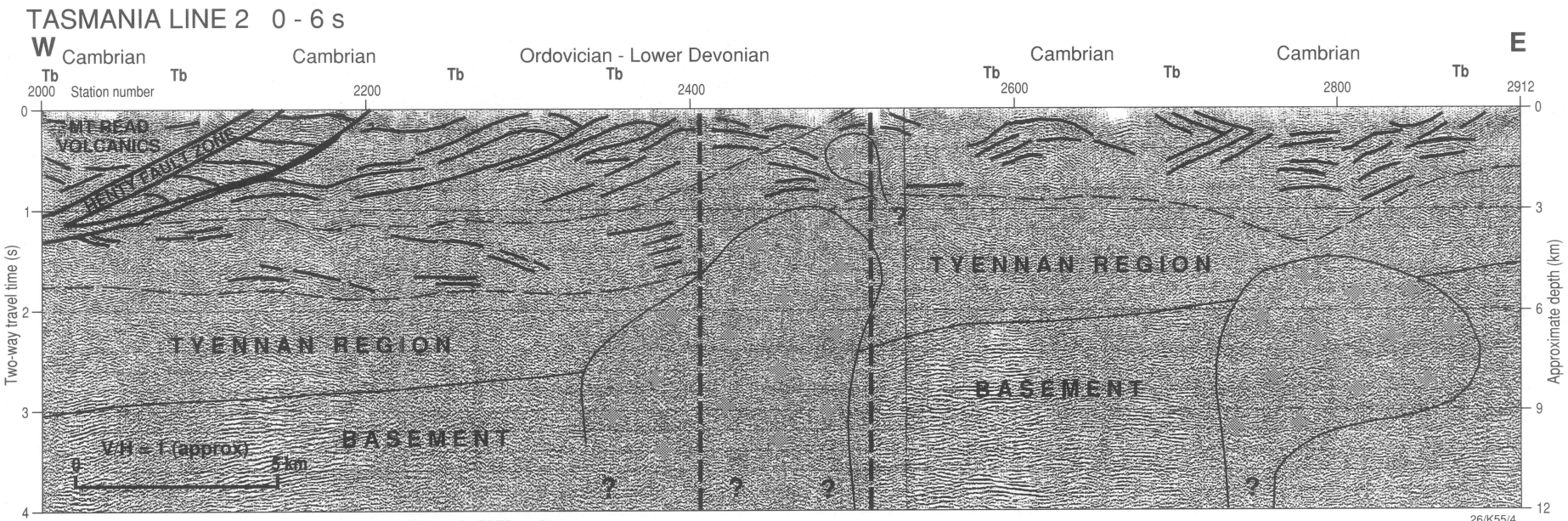


Fig 22 (top). Seismic section of the upper portion of line 1 (V/H = 1).

Fig. 23 (bottom). Seismic section of the upper crust along line 2. The Henty Fault Zone provides a marker on both lines. It has different dips on the two lines owing to the offset along strike of the two lines, and also to a more oblique crossing on line 2. The vertical dotted lines through this figure indicate where the line took two, almost right-angle bends because it had to follow roads in the area (V/H = 1).

# Sources of fluoride in groundwater in north Queensland

M.A. Habermehl[1], J.E. Lau[1], D.E. Mackenzie[2], & P. Wellman[2]

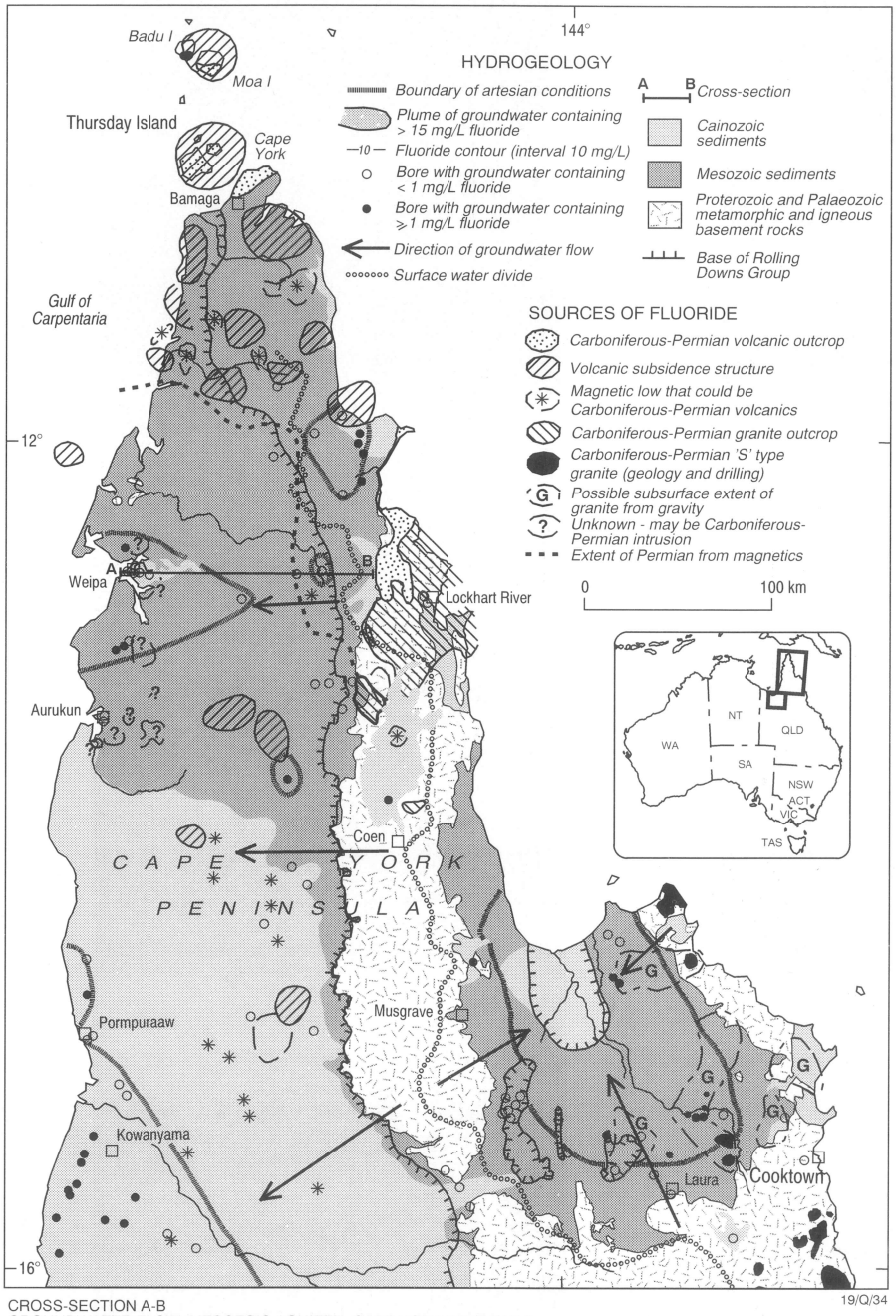


CROSS-SECTION A-B
GROUNDWATER FLOW, MESOZOIC AQUIFER, CAPE YORK PENINSULA

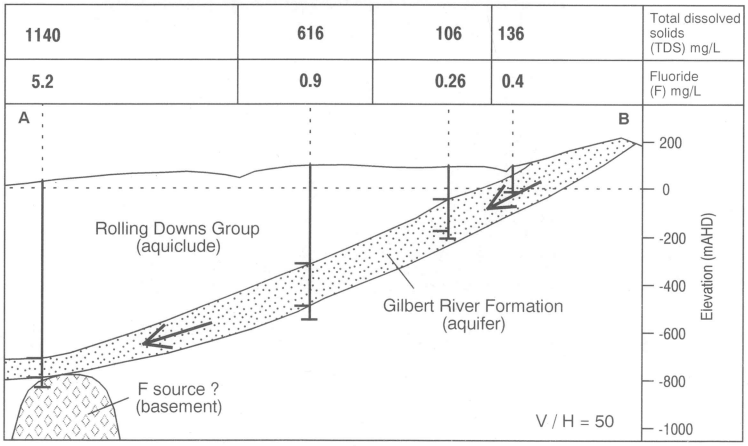


**Groundwater in some parts of north Queensland contains a high proportion of fluoride, which makes it unsuitable for domestic and stock water supplies. High fluoride content in otherwise potable, good-quality groundwater poses a similar problem in other parts of Australia — including portions of the arid zone in central Australia, and regions of the Great Artesian Basin. However, the sources of the fluoride in most areas remain a mystery.**

Analyses of recently acquired groundwater samples in Cape York has detailed the concentration and distribution of the fluoride content. They have confirmed that high fluoride values are widespread in the Mesozoic aquifers of the Carpentaria Basin, are less extensive in the overlying Cainozoic aquifers of the Karumba Basin, and are present in some exposed pre-Mesozoic basement rocks. However, even in the Mesozoic aquifers of Cape York Peninsula, there are still too few deep water-bores to define specific haloes and sources. Groundwater in a high proportion of the water-bores contains more than 1 mg $L^{-1}$ fluoride (Fig. 24).

Regional geological mapping of outcropping Permian–Carboniferous volcanic and intrusive rocks of the North Queensland Igneous Province has shown that some of these rocks, notably those of A-type chemistry, are very fluorine-rich compared with the older basement rocks. Fluorine is present in minerals such as fluorite, topaz, apatite, biotite, and some amphiboles; some of these minerals (notably topaz and fluorite) also occupy fluid or vapour cavities. Vein deposits extremely rich in fluorite are locally concentrated adjacent to some of the A-type volcanic–intrusive complexes. The comagmatic volcanic counterparts of the intrusive rocks generally contain less fluorine because it is both lost with the vapour phase during eruption and removed by circulating fluids during compaction, welding, and subaerial exposure. Even so, any fluorine present in a volcanic pile, especially that in fluorite, will be more accessible to groundwater than that in intrusives because of the much higher permeability of rocks such as tuffs and unwelded ignimbrites. We therefore consider that Permian–Carboniferous igneous rocks,

**Fig. 24. Sources of fluoride in Cape York Peninsula, and groundwater flow in the Mesozoic aquifer (section A–B).**

1 Geohazards, Land & Water Resources Division, Australian Geological Survey Organisation, GPO Box 378, Canberra, ACT 2601; tel. +61 6 249 9426 (MAH), +61 6 249 9703 (JEL); fax +61 6 249 9970; e-mail rhaberme@agso.gov.au, llau@agso.gov.au.

2 Minerals Division, Australian Geological Survey Organisation, GPO Box 378, Canberra, ACT 2601; tel. +61 6 249 9281 (DEM), +61 6 249 9653 (PW); fax +61 6 249 9983; e-mail dmackenz@agso.gov.au, pwellman@agso.gov.au.

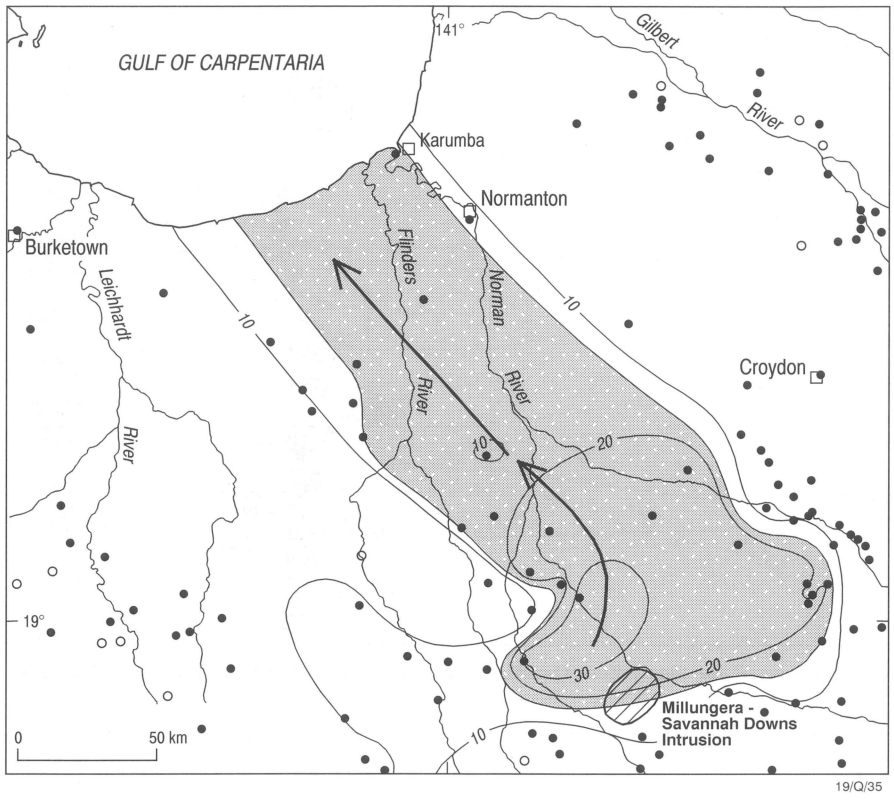


and A-type volcanic rocks in particular, are the most likely sources of fluoride in north Queensland groundwater.

Where available, gravity and magnetic information has facilitated the mapping of concealed Permian–Carboniferous intrusives and volcanic piles in Cape York Peninsula (Fig. 24). The characteristic signature of these bodies is a circular magnetic anomaly superimposed on a gravity low. Circular magnetic anomalies of this type also have been recently recognised beneath the Millungera–Savannah Downs fluoride anomaly in the southern Carpentaria Basin. Earlier drilling of this circular structure has revealed the presence of an A-type granite, typical of those found in the North Queensland Igneous Province (Fig. 25).

We suggest that the association between high-fluoride groundwater, Permian–Carboniferous igneous rocks, and concealed circular magnetic anomalies is a feature common throughout north Queensland, and it should be possible to reduce fluoride risk by using this understanding in the siting of new water-bores.

**Fig. 25. Sources of fluoride in groundwater in the Millungera–Savannah Downs area in the southern Carpentaria Basin (after Queensland Metals Corporation NL, unpublished reports). A key to the symbols is presented in Fig. 24.**

# Further constraints on sequence stratigraphic correlations in the Mount Isa, McNamara, and McArthur Groups

## The Shady Bore Quartzite–Riversleigh Siltstone transition in the 'NABRE'-hood of Riversleigh, northwest Queensland

*Barry E. Bradshaw[1], Andrew A. Krassay[1], M. Jim Jackson[1], Bruce A. McConachie[1], Peter N. Southgate[1], Deborah L. Scott[1], Allan T. Wells[1], & Jan Domagala[2]*

**AGSO and Geological Survey of Queensland personnel examined relationships between igneous rocks and phases of basin development, and measured composite sequence stratigraphic sections, in the following stratigraphic units and areas during the 1996 NABRE ('North Australian basins resource evaluation') project field season, which lasted from late May until early September:**

- Mount Isa Group at Crystal Creek, Paroo Range, and Mount Isa Valley;
- Lower McNamara Group at Gunpowder, Paradise Creek, Police Creek, Barr Hole, and Cararra Range;
- Upper McNamara Group at Lawn Hill, Riversleigh, Musselbrook, Bowthorn, and Cararra Range;
- Fickling Group along the southern flank of the Murphy Inlier;
- McArthur Group (through the Tatoola and Stretton Sandstones, Myrtle Shale, and Emerugga Dolomite) near Cape Crawford; and
- Nathan Group near Cape Crawford.

A major objective of the field season was to constrain the chronostratigraphic surface that coincided with the onset of deformation associated with the hairpin bend (1640 Ma) on the apparent polar-wander path (APWP). On the APWP of Loutit et al. (1994: *in* 'Australian mining looks north — the challenges and choices'. 1994 AusIMM Annual Conference, Darwin, 5–9 August 1994, technical program proceedings, 123–128), this inflection point coincides with magnetic overprint OP2, and probably represents a period of major change in relative plate motion. The unconformity surface was successfully located on top of the Emmerugga Dolomite at a locality 22 km northeast of Cape Crawford. Here, several metres of local relief, and carbonate conglomerate and breccia, mark the surface. Carbonate rocks of the overlying Teena Dolomite contain quartz sand, in marked contrast to the underlying recrystallised dolostones which lack terrigenous components.

### Sequence stratigraphic correlations in the highly prospective Shady Bore Quartzite–Riversleigh Siltstone transition

The NABRE project is developing a regional sequence stratigraphic and structural framework to improve mineral exploration in northern Australia. The recent field season focused attention on the sequence stratigraphy of the transition zone from the Shady Bore Quartzite to the Riversleigh Siltstone (upper McNamara Group) in the area 10 km southeast of Riversleigh homestead, northern Mount Isa. This zone hosts the Grevillea prospect (Coolgardie Gold), and is highly prospective for lead–zinc–silver deposits in black shale of the Palaeoproterozoic lower Riversleigh Siltstone. We use an example from the early results of our 1996 fieldwork to highlight the importance of precise sequence stratigraphic correlations for developing successful mineral plays.

We compare a 450-m section from southernmost Riversleigh, in the Lawn Hill 1:100 000 Sheet (GR 0271910, 7883416; Fig. 26A), with a composite section of 730 m from four sites 5 km farther north (GR 0269766, 7889015; Fig. 26B). The effects of a major marine transgression from Shady Bore Quartzite-type facies (shallow-marine/fluvial sandstones) to Riversleigh Siltstone-like facies (shelf sandstones and siltstones) mark the base of both sections. A maximum flooding surface (labelled A in Fig. 26) in a condensed section of tuffaceous siltstone marks the period of maximum relative water depth and minimum sediment supply. An increase in interbedded sandy siltstone and very fine-grained shelf sandstone suggests a decrease in relative water depth above surface A.

The sharp decrease in gamma-ray counts at surface B (Fig. 26) marks a basinward shift in lithofacies and a sequence boundary. Facies above surface B vary from shallow-marine sandstone at site 5 to fluvial sandstone at sites 1–4. Subsequent transgression resulted in the deposition of marine (tuffaceous) siltstone at maximum flooding surface C. Prograding interbedded shelf sandstone and siltstone accumulated above surface C.

At surface D, a basinward shift in lithofacies from shelf deposits to fluvial sandstone (site 5) and nearshore sandstone (sites 1–4) marks the next sequence boundary. At sites 1–4, interbedded shelf sandstone and siltstone pass upward into a thin layer of green tuffaceous siltstone at maximum flooding surface E. This succession is interpreted

[1] NABRE Research Team, Petroleum & Marine Division, Australian Geological Survey Organisation, GPO Box 378, Canberra, ACT 2601; tel. +61 6 249 9413 (BEB), +61 6 249 9206 (PNS); fax +61 6 249 9956; e-mail bbradsha@agso.gov.au, psouthga@agso.gov.au.

[2] Geological Survey of Queensland, GPO Box 194, Brisbane, Qld 4001; tel. +61 7 237 1503; fax +61 7 235 4074; e-mail dme@mailbox.uq.oz.au.

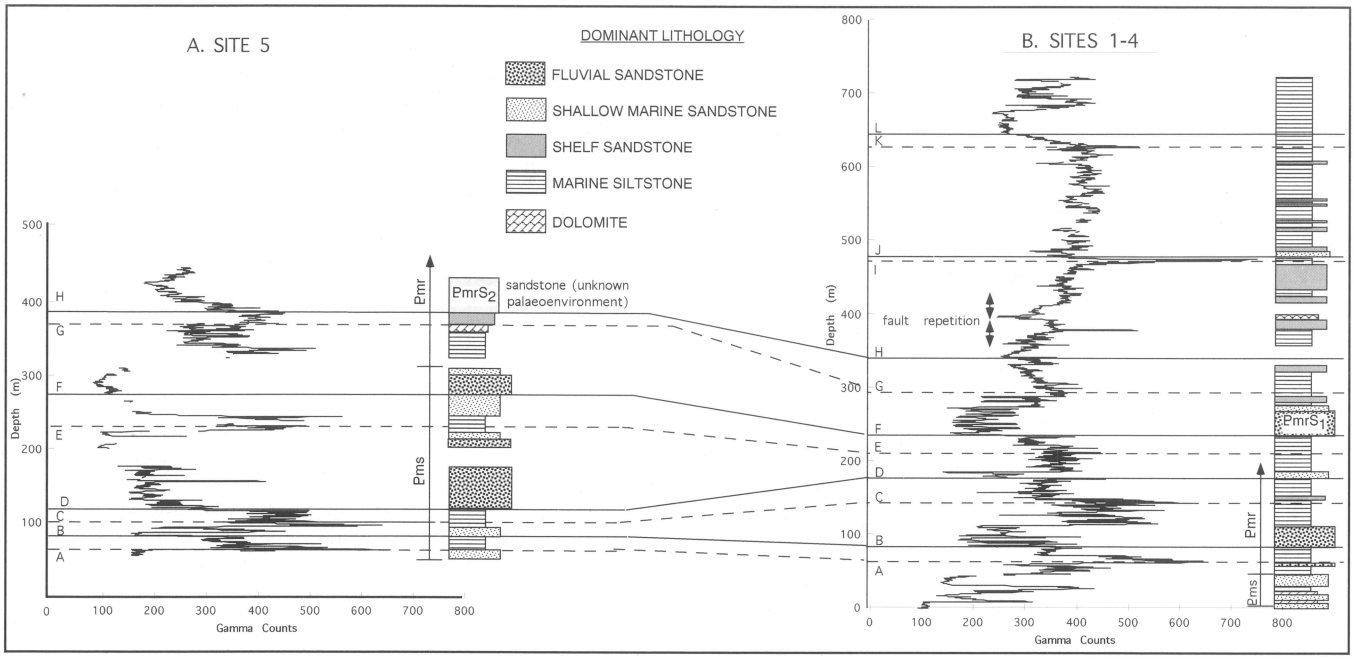


**Fig. 26. Sequence stratigraphic interpretations and correlations of the Shady Bore Quartzite (Pms)–Riversleigh Siltstone (Pmr) transition zone, southern Riversleigh.**

to represent transgression. Lack of diagnostic indicators at site 5 renders palaeoenvironmental interpretation difficult. However, maximum flooding surface E occurs within a thin interval of orange siltstone, interpreted as pro-deltaic in origin.

At sites 1–4 a pronounced erosional unconformity (sequence boundary F) separates interbedded shelf sandstone and siltstone from 60 m of aggradational fluvial sandstone. The change from progradational coastal sandstone to a 30-m-thick interval of aggradational fluvial sandstone marks the same boundary at site 5. In both areas, deep-marine siltstone (tuffaceous and dolomitic at site 5) overlies the fluvial sandstone succession. These transgressive deposits occur beneath maximum flooding surface G. Flaggy to hummocky-cross-stratified shelf sandstone constitutes the overlying progradational system.

Sequence boundary H is the uppermost correlation surface. At site 5, a sharp contact separates massive, thickly bedded sandstone from the underlying thinly bedded and flaggy shelf sandstone. Lateral tracing of this surface identified an erosional unconformity separating the two sandstone lithologies. At sites 1–4, sequence boundary H is poorly exposed, and its position is interpreted from the gamma ray trend. At sites 1–4, shelf sandstone and interbedded siltstone dominate the section between surfaces H–J. Marine siltstone and scattered shelf sandstone beds less than 1 m thick constitute the remaining parts of the succession at sites 1–4.

The overall trend at sites 5 and 1–4 can be divided into two distinct accommodation phases. In the first, between maximum flooding surface A and sequence boundary H, relative water depths fluctuated from shelf to subaerial. During this period, rates of sediment supply were able to match subsidence rates, and this resulted in the deposition of similar facies. A pronounced deepening of the water above sequence boundary H marked the onset of the second accommodation phase. During this period, rates of accommodation increased, and sediment supply rates were insufficient to fill the space being created. As a result, deeper-water shelf deposits accumulated in place of the coastal-plain facies.

## Implications of the foregoing correlations for mineral exploration

Developing a detailed sequence stratigraphic framework such as the one described in this example facilitates a detailed understanding of basic architecture, the type of information necessary to enhance mineral exploration strategies.

- Sediment-hosted mineral deposits in the Mount Isa basin are usually found in black (organic-rich) shale and dolomitic siltstone horizons closely associated with condensed intervals and maximum flooding surfaces. Sequence stratigraphy predicts where such condensed intervals occur (surfaces A, C, E, and G in Fig. 26).
- Sediment-hosted mineral deposits are often associated with distinct regional tectonic events. The HYC lead–zinc–silver deposit in the McArthur Basin occurs in black dolomitic siltstone formed within pull-apart basins during a major hairpin in the APWP. Using regional sequence stratigraphic correlations, we associate the Shady Bore–Riversleigh transitional phase with this same regional tectonic event.
- Fluid-flow histories of sediment-hosted mineral deposits often begin with hot oxidising brines migrating along faults during major tectonic events. Subsequent mineralisation requires reaction with a reducing agent (e.g., hydrocarbons or organic-rich sediments) within a potential reservoir. Sequence stratigraphy improves our understanding of the three-dimensional geometry of sedimentary rocks, and helps predict where the necessary combination of sources for reducing agents, migration fairways, reservoir rocks, and seals will occur.
- Sequence stratigraphy is vital for accurate regional correlations of a known productive horizon. For example, the condensed section associated with maximum flooding surface A at sites 1–4 has the combination of lithology, age, proximity to faults, and surrounding reservoir rocks that is commonly associated with an economic mineral deposit. However, horizons A–F at site 5 occur within mapped Shady Bore Quartzite (Pms), and within mapped Riversleigh Siltstone (Pmr) at sites 1–4. If standard lithostratigraphic mapping techniques were applied, the hypothetical mineral deposit at horizon A at sites 1–4 would be incorrectly tied to and searched for at horizon H at site 5. Sequence stratigraphy is therefore of critical importance to successful exploration for sediment-hosted mineral deposits in the Palaeoproterozoic Mount Isa basin.

*Continued from opposite page.*

biodegraded because they were protected from meteoric groundwaters by intraformational seals.

## Keyling–Hyland Bay petroleum system

Gas flows from the Hyland Bay Formation at Tern, Fishburn and Penguin, and gas with minor condensate at Petrel, are believed to have been sourced from Permian deltaic sediments. Geochemical analyses of the condensate from Petrel 4 shows that it has a diagnostically heavy carbon isotopic signature ($\delta^{13}$Csat = –24‰) consistent with its generation from mature Permian clay-rich source rocks containing a mixture of land-plant and marine algal material. Source-rock data suggest two likely organic-rich Permian intervals:

- Early Permian delta-plain coal and marginal-marine shale of the Keyling Formation (mean TOC = 35.2%, mean HI = 230 mg $S_2$/gTOC for coaly rocks; mean TOC = 2.8%, mean HI = 95 mg $S_2$/gTOC for shale); and
- to a lesser extent, Late Permian prodelta shale of the Hyland Bay Formation (mean TOC = 2%, mean HI = 55 mg $S_2$/gTOC); better source quality for the Hyland Bay Formation may occur in the Petrel Deep, outboard of the Petrel and Tern fields.

Burial-history models in the central Petrel Deep (Fig. 32) suggest that both the Keyling and Hyland Bay source intervals expelled the bulk of their gas in the Late Cretaceous, but that oil and minor gas were also expelled from the older Keyling source interval during or immediately after trap formation associated with the Middle Triassic–Early Jurassic (Ladinian–Carnian) Fitzroy Movement (Fig. 31). The gas–condensate accumulations at Petrel could thus be sourced from either or both Permian intervals. On the shallower flanks of the Petrel Deep, however, expulsion of oil and gas from the Keyling interval postdated the Fitzroy structuring. Thus, combined stratigraphic–structural plays on the northeast flank of the sub-basin, where Kinmore 1 and Flat Top 1 demonstrated significant source potential of the Keyling Formation, represent the best prospects for liquid hydrocarbons within the Permian Keyling–Hyland Bay petroleum system.

*Continued from back page.*

Three petroleum systems are defined:

- Ningbing–Bonaparte (Larapintine 3);
- Milligans (Larapintine 4); and
- Keyling–Hyland Bay (Gondwanan).

Liquid hydrocarbons generated from these systems can be readily differentiated by their carbon isotopic signatures (Fig. 28).

## Ningbing–Bonaparte petroleum system

Oils attributed to this system have a marine carbonate source signature, and are probably sourced from the Late Devonian Ningbing and Bonaparte Formations. They are restricted to mineral and petroleum wells in the onshore Petrel Sub-basin. This system offers limited potential due to poor reservoir development and quality, poorly known source kitchens, and high preservation risk for hydrocarbons that were probably expelled in the Early Carboniferous (Visean–Namurian).

## Milligans petroleum system

Oils from the Milligans petroleum system have been recovered onshore at Waggon Creek 1 well in the Milligans Formation, and offshore at Barnett 1 and 2 and Turtle 1 and 2 in Milligans and overlying younger Carboniferous–Permian reservoirs (Fig. 32). These oils are characterised by light carbon isotopic values (mean $\delta^{13}$Csat = –28‰), pristane/phytane and $C_{27}/C_{29}$ sterane ratios of just below unity, an abundance of diasteranes, diahopanes, tri- and tetracyclic terpanes (Fig. 29), and minor gammacerane and 28,30-dinorhopane. Severe biodegradation has altered the composition of many of the shallower oils recovered at Barnett and Turtle, resulting in an overprint of 25-norhopanes. These oils have been correlated with anoxic marine mudstones of the Early Carboniferous Milligans Formation.

The most organic-rich and least mature rocks analysed to date in the Milligans Formation (mean TOC = 2.8%, mean HI = 204 mg $S_2$/gTOC) occur in the mineral hole NBF1002. Sequence stratigraphic analysis indicates that the richest organic intervals penetrated by petroleum exploration wells generally occur in the upper portion of a second-order transgressive systems tract near the middle of the Milligans supersequence. However, no wells have penetrated what is probably the most promising source interval located beneath downlapping progradational highstand clinoforms in the offshore Cambridge Trough immediately south of the Turtle–Barnett High (Fig. 32). This source interval may also occur within the lobe of the Milligans supersequence immediately north of the Turtle–Barnett High. Interpreted basin-floor fans and stratigraphic pinch-out of turbiditic sandstone against the basal Milligans sequence boundary offer untested exploration plays in the Cambridge Trough, and so do upper-slope carbonate mounds in the overlying Tanmurra supersequence in the area north of the Turtle–Barnett High.

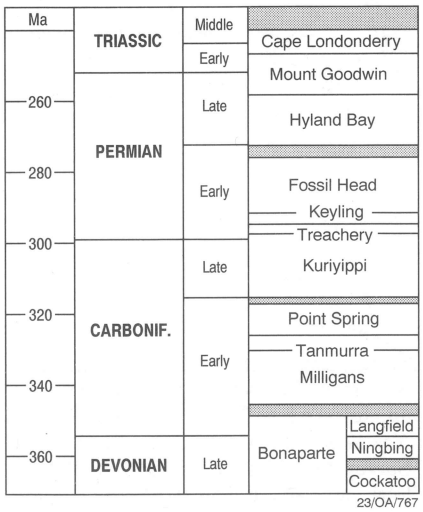


**Fig. 27. Ages of late Palaeozoic sequences in the Petrel Sub-basin.**

Burial-history modelling suggests that hydrocarbons were expelled from the mid-Milligans source kitchen north of the Turtle–Barnett High in the late Early Carboniferous (Namurian; Fig. 30, A), before the regional Treachery Shale seal was emplaced in the Early Permian. In contrast, expulsion from the source kitchen in the Cambridge Trough to the south of the Turtle–Barnett High occurred in the Early Permian (Fig. 30, B), immediately after emplacement of the regional seal. Jefferies (1988: *in* Proceedings of the Petroleum Exploration Society of Australia North West Shelf Symposium, Perth, 563–569) observed the occurrence of composite biodegraded and non-biodegraded oils in Turtle 1, and concluded that they formed from two phases of migration. The severe biodegradation of the first phase before the emplacement of the second phase is readily explained by this expulsion history. Oils expelled from the northern kitchen were biodegraded as they migrated into shallow fluvial/deltaic reservoirs under oxidising conditions, whereas oils expelled from the southern source kitchen accumulated in now more deeply buried reservoirs which were sealed from oxidising groundwaters by the Treachery Shale. Subsequent fault reactivation associated with the Fitzroy Movement probably resulted in partial breach of this seal, and a second phase of oxidation and biodegradation of the shallower accumulations. In contrast, any hydrocarbon accumulations within stratigraphic traps to the north and south of these highs would not have been

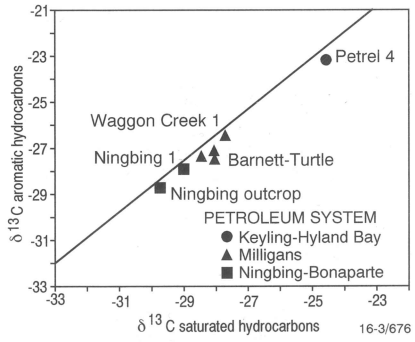


**Fig. 28. Carbon isotopic signatures of liquid hydrocarbons.**

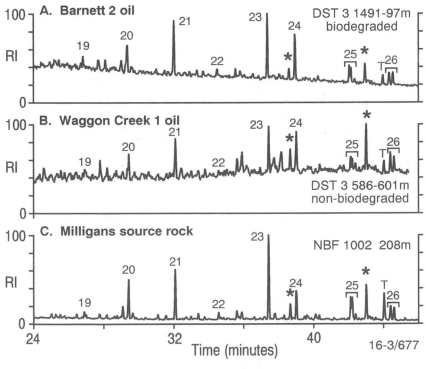


**Fig. 29. Reconstructed ion chromatograms showing tri- and tetracyclic terpanes in oils recovered from Barnett 2 and Waggon Creek 1, compared with Milligans organic-rich rocks in mineral hole NBF1002. Numbered peaks refer to carbon number of tricyclic terpanes; T denotes $C_{24}$ tetracyclic terpane; and * denotes as yet unidentified peaks which are diagnostic of the Milligans petroleum system.**

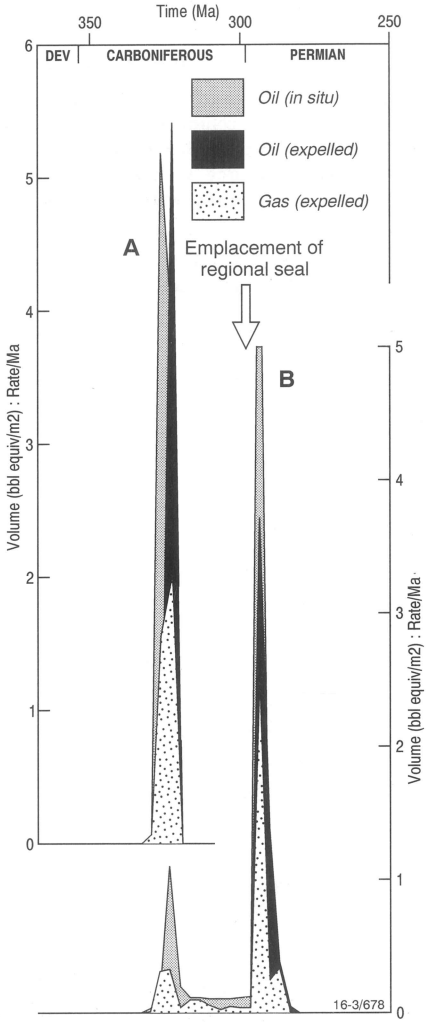


**Fig. 30. Hydrocarbon generation plot of the inferred mid-Milligans source interval at hypothetical well sites in source kitchens (A) north and (B) south (Cambridge Trough) of the Turtle–Barnett High.**

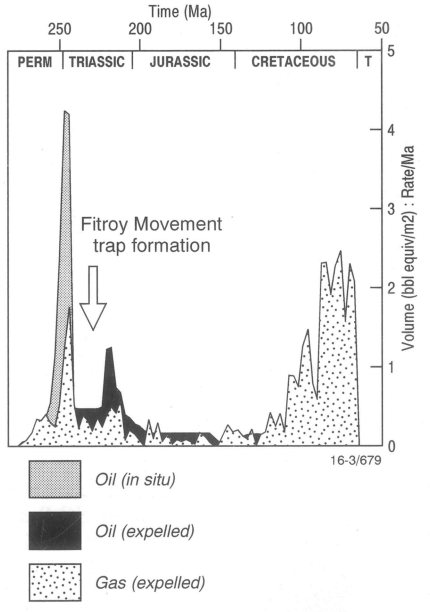


**Fig. 31. Hydrocarbon generation plot of the inferred Keyling source interval below TD at Petrel 2.**

*Continued on opposite page.*

# Source and generation history of Palaeozoic hydrocarbons, Petrel Sub-basin

*Dianne Edwards[1], John M. Kennard[1], James B. Colwell[1], & Peter J. Jones[1]*

**As part of its recently concluded Petrel Sub-basin study (a component of the 'North West Shelf' project), AGSO has integrated structural, sequence stratigraphic, and biostratigraphic data with geochemical (Rock-Eval pyrolysis, biomarker, and isotope) analyses of oils and organic-rich rocks to define the source and generation history of hydrocarbons within the sub-basin. The largely Palaeozoic Petrel Sub-basin forms the southern part of the Bonaparte Basin in northwestern Australia (Figs. 32 and 27). It contains two large undeveloped gas fields (Petrel and Tern), and oil and gas shows have been recorded in numerous wells.**

*Continued on p. 23*

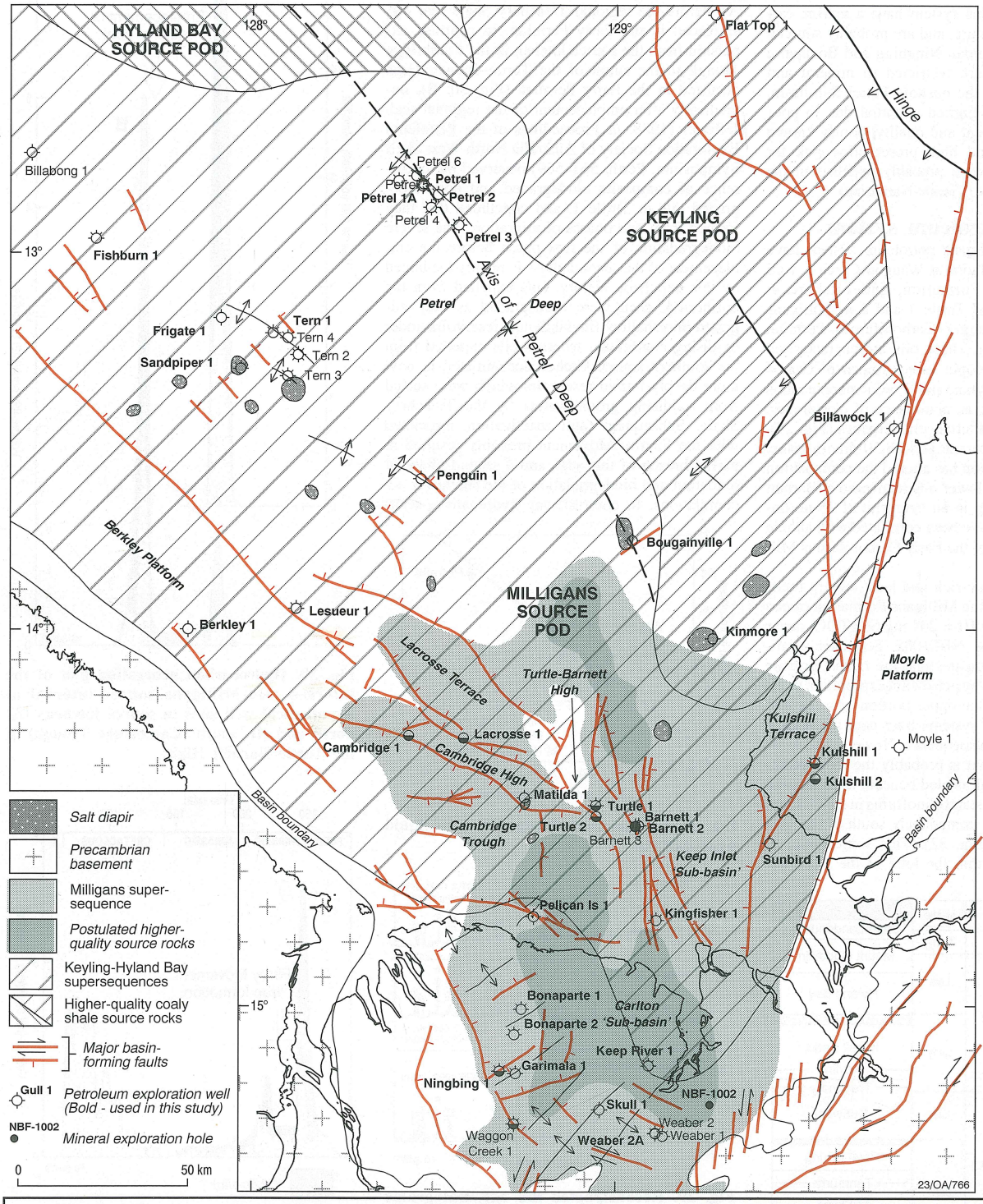


**Fig. 32. Distribution of potential source units, and probable richer source-rock intervals (dense hatching), in the Early Carboniferous Milligans and the Permian Keyling–Hyland Bay petroleum systems.**

[1] Petroleum & Marine Division, Australian Geological Survey Organisation, GPO Box 378, Canberra, ACT 2601; tel. +61 6 249 9782 (DE), +61 6 249 9204 (JMK), +61 6 249 9346 (JBC), +61 6 249 9737 (PJJ); fax +61 6 249 9956; e-mail dedwards@agso.gov.au, jkennard@agso.gov.au, jcolwell@agso.gov.au, pjones@agso.gov.au.

The *AGSO Research Newsletter* is published twice a year, in May and November. For further information please contact AGSO's Spatial Information & Mapping Services group, tel. +61 6 249 9111 (extn 9623), fax +61 6 249 9982. Correspondence relating to the *AGSO Research Newsletter* should be addressed to Geoff Bladon, Editor, *AGSO Research Newsletter*, Australian Geological Survey Organisation, GPO Box 378,cnr Constitution Avenue & Anzac Parade, Parkes, Canberra, ACT 2601; tel. +61 6 249 9111, extn 9249; fax +61 6 249 9990, e-mail gbladon@agso.gov.au.

 ISSN 1039-091X PP255003/00266